Cognitive effort and reward. Functional imaging of time on task and the involvement of dopaminergic and cholinergic substrates

Chiara Orsini[1*], Julia Bosch[2], Karin Labek[1], Roberto Viviani[1,2*]

1 Institute of Psychology, University of Innsbruck, 6020 Innsbruck, Austria

2 Department of Psychiatry and Psychotherapy III, University of Ulm, 89075 Ulm, Germany

*** Corresponding authors**

Abstract

Neuroimaging studies have identified the neural substrates associated with sustained cognitive efforts and control and their modulation by rewards. Different lines of evidence implicate the prefrontal cortex (especially the anterior cingulum, ACC), dopaminergic, and cholinergic substrates in this modulation. We studied here the activity of these substrates at increasing time on task (providing increasing levels of cognitive effort) in trial blocks with differing reward levels. In the cortex, while peaking in the ACC, activity associated with time on task was extensive, also including activity decrements outside the default mode network, primarily involving motor and somatosensory regions. Information about reward levels was carried in the ventral striatum, consistent with its motivational role, but did not reflect trade-offs with increasing efforts during time on task. Instead, the ventral tegmental area and parts of the basal forebrain (BF) corresponding to the cholinergic Ch4 nuclei increased in activity with time on task and were sensitive to reward levels. This BF activity is consistent with a cholinergic role in driving compensatory efforts modulated by reward levels. These findings identify the BF as a neuroimaging phenotype associated with sustaining task sets and cognitive efforts.

Cognitive effort and reward. Functional imaging of time on task and the involvement of dopaminergic and cholinergic substrates

Introduction

Sustained attention (Davies & Parasuraman, 1982; Mackworth, 1948, 1950; Parasuraman & Davies, 1984) is conceptualized as the cognitive capacity required to remain task-focused over a prolonged time (Coull, 1998; Oken et al., 2006; Timmers, 2014; Warm et al., 2008). A common observation, also based on experience, is that this requires effort, and that performance may worsen with time (Warm et al., 2008). The term "vigilance" is sometimes used in this context, although with less specificity, often also referring to the arousal state (Oken et al., 2006), which may degrade with prolonged time on task. However, Posner and Boies (1971) argued that sustained attention is involved during relatively brief tasks, a view supported by meta-analytic evidence on its recruitment already after ten seconds of work (Langner & Eickhoff, 2013). Here, we use the notion of sustained attention to refer to effortfully and continuously attending to a short and simple task with low or no working memory load, without considering the additional burden of mental fatigue and exhaustion arising from several minutes or hours of labor.

The present functional imaging study aims to investigate the neural correlates of sustained attention and the effect of reward levels on these potential correlates by looking at the effects of the temporal dimension ("time on task") while also considering the possible involvement of dopaminergic, noradrenergic, and cholinergic substrates. This focus addresses issues raised in separate strands of theory and evidence in the literature on sustained attention and cognitive effort and their modulation by reward, possibly referring to interrelated mechanisms. To our knowledge, these separate strands have never been investigated within the same framework in humans.

Early empirical investigations of the notion of effort took place within the context of bottleneck or limited resources models of controlled processes more generally (Kahneman, 1973). More recently, the notion of effort has been used to model mechanisms that modulate recruitment of cognitive control (Shenhav et al., 2017). Abundant empirical evidence demonstrates that cognitive efforts are avoided in the presence of alternatives, suggesting that cognition internally maintains a representation of its own costs (Kool et al., 2010; Mcguire & Botvinick, 2010). This notion is also consistent with the observation that rewards attached to the correct execution of tasks affect the levels of effort associated with attentional demands and improve performance (for a review of the extensive neuroimaging evidence, see Botvinick & Braver, 2015), as if rewards were traded off with the costs of cognition for their procurement. This trade-off is apparent also in sustained attention tasks, as perceived effort during continued performance is less when the benefits associated with it are greater (Boksem & Tops, 2008). Among all areas activated by executive control, it has been proposed that the anterior cingulate (ACC) is concerned with evaluating the allocation of cognitive effort based on a computation of costs and benefits based on evidence from experiments in laboratory animals (Walton et al., 2006) and neuroimaging studies in man (Shenhav et al., 2017). Many findings in the literature on ACC recruitment are explained by the resulting model, which predicts higher activity in

ACC with higher cognitive demands and higher reward levels (Shenhav et al., 2016; Shenhav et al., 2017).

In the present experiment, a simple detection task was modulated by varying levels of reward (Viviani, Dommes, Bosch, Steffens, et al., 2020). A cue, announcing the level of reward obtained by performing the task correctly, was followed by a "foraging patch" block of about 15s, where participants had to press the right or the left button each time a stimulus appeared at the right or left side of the screen to collect the announced reward (Figure 1A). Previous characterizations of this task (Viviani, Dommes, Bosch, Steffens, et al., 2020) have shown activity of the ventral striatum depending on the lack of predictability of the valence of the cue, as in well-known prediction error models of dopamine signaling (Montague et al., 1996; Schultz, 1998) and as in numerous previous neuroimaging studies (Abler et al., 2006; Berns et al., 2001; Li et al., 2006; McClure et al., 2003; O'Doherty et al., 2003; Rutledge et al., 2010; Seymour et al., 2007; Tobler et al., 2006). The foraging patch, in contrast, carries no prediction error, but is characterized by different levels of reward accruing from doing the task. Reward levels in the foraging patch were associated with activity in the ventral tegmental area/substantia nigra (VTA/SN), as well as in the nucleus accumbens (NAcc, Figure 1B).

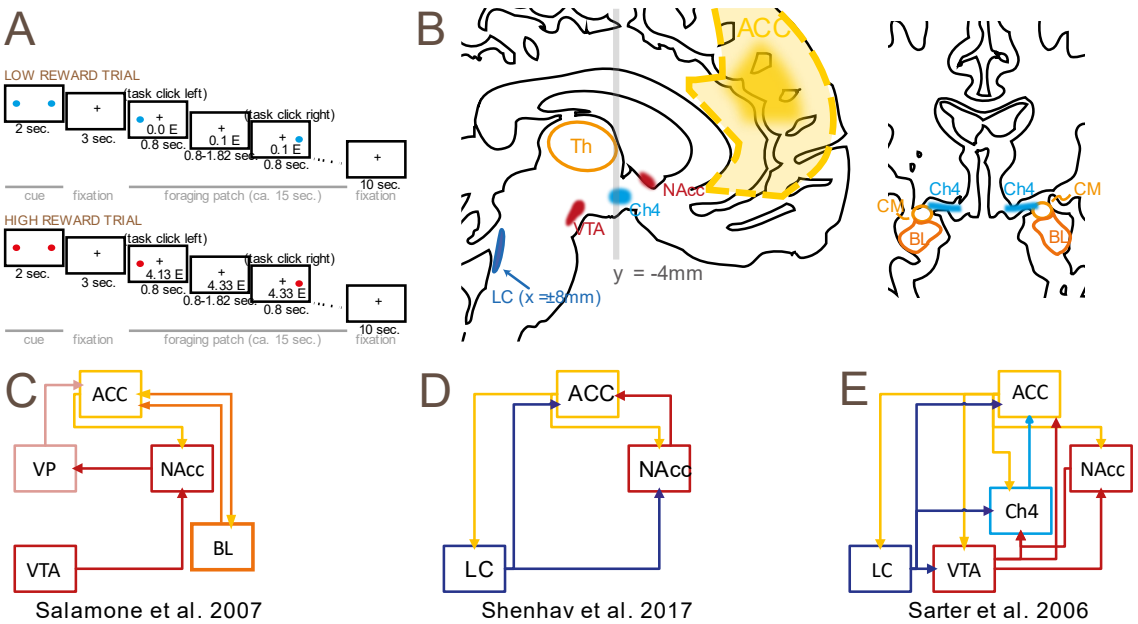

Figure 1: A: Schematic representation of the paradigm of the study, consisting of trial blocks with high and low reward levels ("foraging patches", in blue and red in the figure). A linear trend within the foraging patches indexed time on task (modified from Viviani, Dommes, et al., 2020). B: Brain structures involved in models on the interaction between reward and cognitive efforts. C: In the motivational model, redrawn from Salamone et al. (2007), dopaminergic substrates (NAcc and VTA) energize cognition through modulatory activity in cortex together with the basolateral amygdala (BL), with a preferential distribution to prefrontal areas through the intermediation of the ventral pallidum (VP). D: In the model of the computation of required effort by Shenhav et al. (2017), the ACC signals increased effort requirements to the locus coeruleus (LC) and the nucleus accumbens (NAcc), which modulate cortical activity. E: Cholinergic model of cognitive modulation from the animal literature, redrawn from Sarter et al. (2006). Cholinergic modulation (Ch4) flanks the modulation from LC and dopaminergic substrates. CM: centromedial amygdaloid nucleus.

By tracking a signal of the reward expected from work, activity in dopaminergic regions during the foraging patch may represent the benefit of allocating cognitive control and the motivational effects of reward (Viviani, Dommes, Bosch, Steffens, et al., 2020) consistently with well known models of the motivational role of dopamine (Figure 1C). In turn, the effort associated with sustained attention may increase during the progression of the foraging patch,

representing increasing costs of control. The present study focuses therefore on time-on-task effects in the foraging patch (which to date have not been looked at in this task) using a database of N=415 individuals that completed this task in the scanner (Viviani, Messina, et al., 2020). We expected to replicate the involvement of the sustained attention cortical network reported in the literature (Langner & Eickhoff, 2013) and the key role of ACC in registering changes in reward levels and cognitive demands in time on task (Shenhav et al., 2017). However, the study also gave us the opportunity to investigate the role of subcortical nuclei mentioned in literature on cognitive effort and reward.

One question was the change in activity of VTA/SN and NAcc during time on task. Several proposals have been made about the nature of cognitions costs (Shenhav et al., 2017), but in the case of prolonged but simple tasks a possible contributor may be "opportunity costs" (Kurzban et al., 2013), i.e., the notion that remaining on the same task for a long time implies forfeiting returns that may be obtained with less effort elsewhere, a computation not unlike the one formalized by foraging models (Kurzban, 2016). Previous neuroimaging studies have shown that activity in dopaminergic substrates is decreased by cognitive efforts to obtain rewards (Botvinick et al., 2009; Kurniawan et al., 2013), although the animal literature is not supportive of this finding (Walton & Bouret, 2019). Here, we hypothesized that VTA/SN and NAcc, activated here by levels of reward, would also track the diminishing net value of the rewards during the sustained attention period.

A further issue discussed in the neuroimaging literature on the ACC concerns the recipients of its output, an issue related to the mechanisms through which control is modulated. A working hypothesis is the involvement of the locus coeruleus (Shenhav et al., 2017), due to evidence on its role in modulating attention (Aston-Jones et al., 1994; Usher et al., 1999). In this literature, this model also includes ACC receiving input from the anterior insula to implement increased cognitive engagement (Shenhav et al., 2016; Shenhav et al., 2017).

However, in the animal literature simple signal detection tasks have also provided abundant evidence that cholinergic activity from the Ch4 region in the basal forebrain (BF) (Mesulam, 2004; Mesulam, 2013; Mesulam et al., 1983) mediates sustained attentional performance (for reviews, see Sarter et al., 2001; Sarter & Bruno, 2002; see also Broussard, 2012). Cortical cholinergic activity increases in cases of "cognitive challenges", when distractors are introduced or during time on task, and is thought to compensate for the possible reduced attentional performance during these challenges and to be key to the instantiation of cognitive effort (Sarter et al., 2006). Interestingly, the animal literature has also provided evidence of the sensitivity of the cholinergic BF to reward contingencies (Hangya et al., 2015; Richardson & DeLong, 1986), providing yet another possible avenue for the computations involved in efforts to sustain attention (Figure 1E).

Our study provided two novel insights. The first was that, while the expected cortical activations associated with cognitive effort were replicated in the data, a sample of this size also provided evidence (at voxel-level correction) that most of the cortex was modulated by time on task in one way or another. In our data, the cortical activations reported in the literature looked like the tip of the iceberg and were opposed to isolated decrements of activity with time on task, not located within the default mode network.

The second was that cholinergic BF and VTA were active and modulated by reward in a manner dissociated from NAcc. There were no effects in the brainstem in the location of the locus coeruleus. This finding suggests that, in a very simple task, cholinergic activity may play an important role in the maintenance of the task set in humans, while the motivational value of reward is tracked by a signal emerging in the ventral striatum.

Results

Behavioral data

Behavioral data were reported in Viviani, Messina, et al. (2020). Briefly, participants could carry out the task with ease (giving the correct response in over 99% of targets). After adjusting for the first trial in block, where participants were significantly less accurate (z = -7.9, p < 0.001), correct responses diminished with the time on task (z = -4.2, p < 0.001). The reward amount influenced accuracy as well, with worse performance in the less rewarding condition (z = -3.6, p < 0.001).

Reaction times (RTs) were shorter in high reward forage blocks by about 3.2ms (t = 9.1, p < 0.001). After adjusting for the first trial, which was slower than the subsequent trials (of about 84.6ms, t = 117.5, p < 0.001), RTs showed increases during the forage block, i.e., a time on task effect (about 0.3ms per trial, t = 4.5, p < 0.001). The significance of the time on task effect was robust to variations of the model.

For details, see the Supplementary Materials.

Neuroimaging data

In the following, 8 mm smoothing was used to analyze cortical effects and in the tables in the Appendix. In the text, we report on an analysis at 4 mm smoothing for effects in subcortical nuclei and the amygdala. In both cases, significance levels were corrected at voxel level (peak level) for the whole brain volume.

Effect of reward during the forage phase

The main effects of reward levels were described in Viviani, Dommes, Bosch, Steffens, et al. (2020); Viviani, Messina, et al. (2020). The effects were replicated here. Briefly, the effect of reward in the forage phase showed an involvement of VTA/SN (x, y, z: 7, -13, -10, t = 6.66, p < 0.001 voxel-level corrected), and of the NAcc (x, y, z: -7, 5, -4, t = 9.46; and 6, 5, -4, t = 7.84, all p < 0.001 voxel-level corrected). Of note, no effect of reward was observed in the Nucleus Basalis of Meynert (NBM)/Ch4 or the locus coeruleus in this contrast.

Effect of time on task

The effect of time-on-task was modelled by the linear time during the forage blocks, when participants executed target detection continuously. This model revealed widespread cortical and subcortical activity increases with increased time on task (Table A1; Figure 2, red-yellow colors). The largest cluster was localized in prefrontal areas (both medial and dorsolateral), and extended to parietal, temporal, occipital, and subcortical regions.

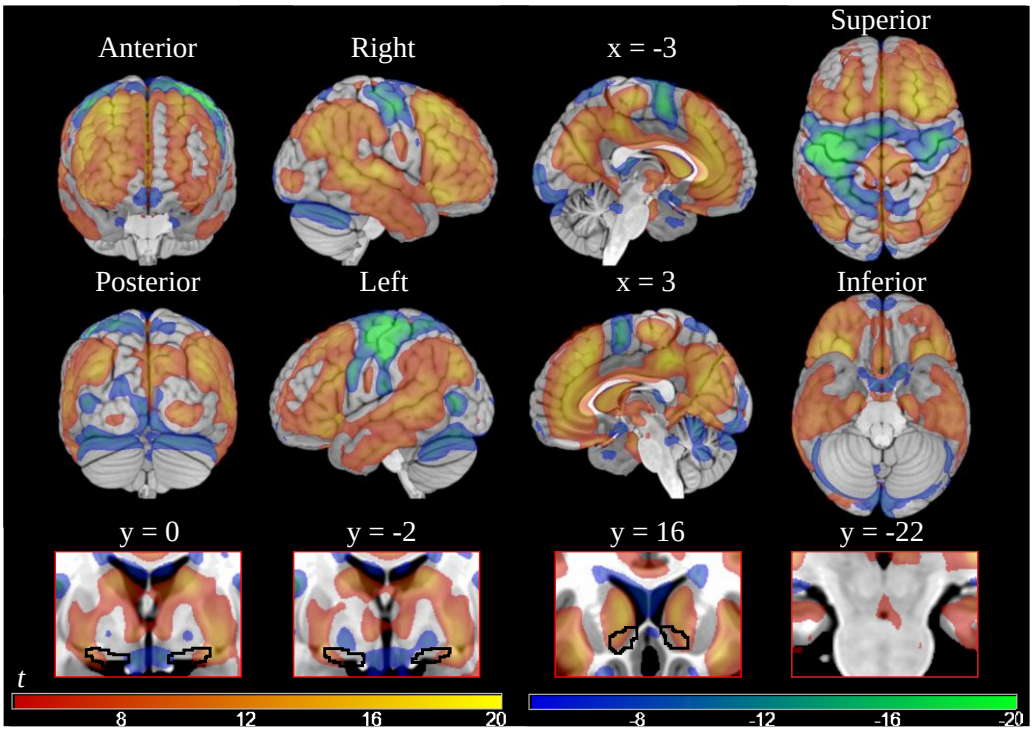

Figure 2: On the top, parametric maps of voxel-level significant cortical activations and deactivations associated with increasing time spent on task (smoothing = 8 mm). On the bottom, subcortical significant activity (smoothing = 4 mm) in Ch4 (y = 0; y = -2), NAcc (y = 16), and VTA/SN (y = -22). Areas showing an activity increase are the ones in the red-yellow gradient; areas showing an activity decrease are the ones in the blue-green gradient. T-values = ±4.5/±20.

Some cortical substrates showed activity decreases with the time spent on the detection task (Table A2 and Figure 2, blue-green colors). Particularly, the areas showing this pattern bilaterally (even though presenting a stronger deactivation in the left hemisphere) were the premotor/motor and somatosensory cortices, and the left associative visual cortex. In separate analyses (not shown here for brevity), we verified that these decreases were present in models without adjustment for "physiological noise" confounders.

In subcortical regions, increases in activity with time on task included the basal ganglia, the thalamus (x, y, z: 6, -10, 6, t = 10.73), the central nucleus of the amygdala (centromedial amygdaloid area, x, y, z: 25, -1, -11, t = 14.09, and -24, -1, -11, t = 11.81), the lateral portions of the cholinergic Ch4 NBM component (x, y, z: 24, -1, -10, t = 13.20, and -22, -1, -11, t = 11.61), the VTA/SN (x, y, z: 3, -16, -10, t = 8.63), and the NAcc (x, y, z: -12, 15, -4, t = 12.48, and 13, 17, -5, t = 10.82; all at voxel-level significance $p < 0.001$ with 4 mm smoothing; see the bottom row of Figure 2). Hence, the subcortical areas that we hypothesized as being related to time on task were significantly involved. However, the changes in VTA/SN and NAcc activity over time were in the opposite direction as in our *a priori* hypothesis (which was that in dopaminergic substrates activity would decrease). Furthermore, activity in the NAcc and Ch4 was embedded in a large activation blob, making evaluation of its specificity more difficult. NAcc, for example, was part of a general activation of the caudate. In subcortical regions, time on task was associated with activity decreases in the pallidum (x, y, z: -15, -4, -8, t = -12.67, and 16, -2, -7, t = 9.58; voxel-level significance $p < 0.001$ with 4 mm smoothing, see insets in the bottom row of Figure 2 at y = 0 and -2).

Interaction time on task x reward level

The interaction between time on task and reward levels (Table A3; Figure 3, red-yellow colors) revealed a mostly right-lateralized pattern of activation in areas that were recruited also in the

time on task analysis. Hence, in the major cortical areas where activity increased during time on task it did so more in high reward trials, although this effect was more markedly right-lateralized. A notable exception to this lateralization pattern was ACC/medial prefrontal cortex, where the highest effects of the interaction were reached (black asterisk in Figure 3 at $x = 3$).

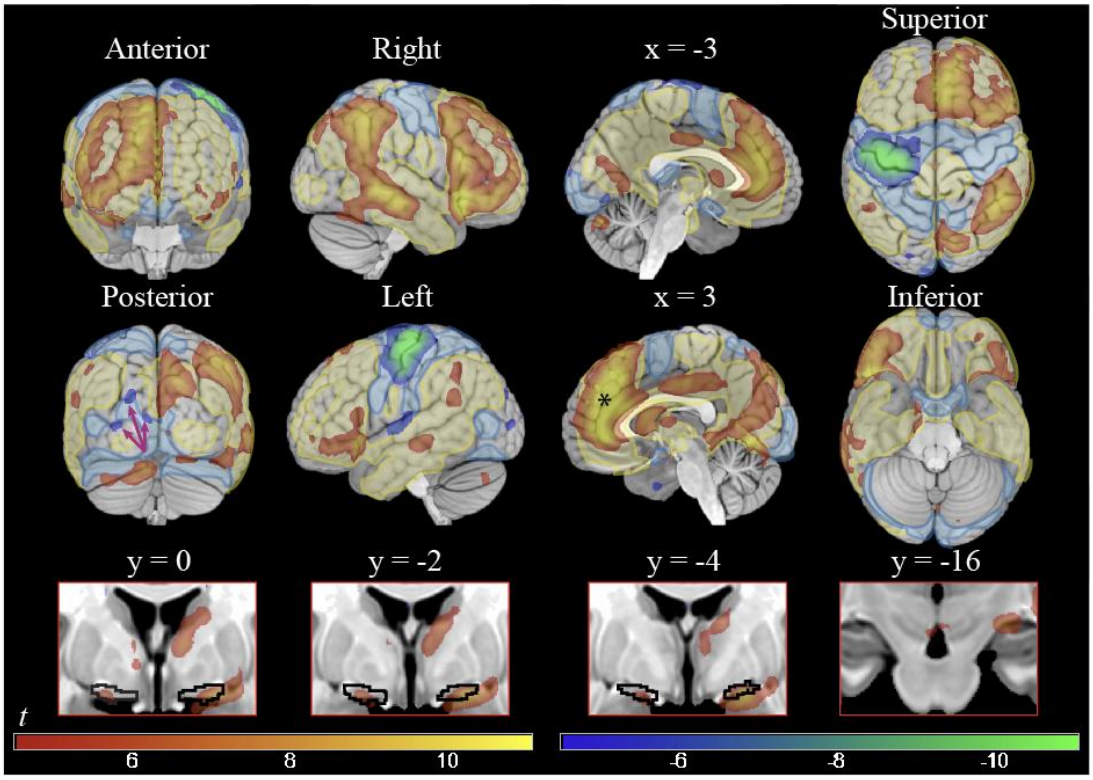

Figure 3: On the top, cortical voxel-level significant parametric maps of the positive and negative interaction between time on task and levels of reward (high reward vs low reward) (smoothing = 8 mm). On the bottom, subcortical significant activity (smoothing = 4 mm) in Ch4 (y = 0; y = -2; y = -4), and VTA/SN (y = -16). Areas shown in red-yellow presented greater activity during time on task in high than in low reward conditions; interaction in the other direction is shown in the blue-green one. T-values = ±4.5/±11. In shaded yellow and blue cortex, positive and negative activations in the time on task of Figure 2, showing that areas modulated by reward in the interaction were mostly a lateralized subset of the time on task effects. The black asterisk at the sagittal slice at *x* = 3 shows the peak effect of the interaction at *y* = 41, *z* = 23.

In the opposite direction, more marked decreases in time on task during high reward trials involved an almost totally left-lateralized set of fronto-parietal areas (Table A4; Figure 3, blue-green colors), which overlapped with the fronto-parietal deactivations in the time on task contrast. Also, the superior occipital cortex showed significant decreases (arrows in the posterior view in Figure 3).

While not as extensive as in the time on task contrast, also the interaction with reward involved large cortical regions with internal peaks of activity. To visualize these peaks, in Figure 4A we show the interaction at a very high threshold level. In Figure 4B and C we show the areas of connectivity and co-activation of the seed of the ACC peak, taken from the Neurosynth database (www.neurosynth.org), showing that in both our data and in the database, ACC was connected with the other peaks, including that of the anterior insula. In both connectivity and data are also co-activations in the middle temporal gyrus and inferior parietal lobe. In panel D, the decoding analysis from the Neurosynth database revealed that these areas were active in many studies in the literature involved with cognition, where the association referred to cognitive conflict, although the strongest overlap involved social cognition tasks, seemingly driven by the ACC and inferior parietal effects.

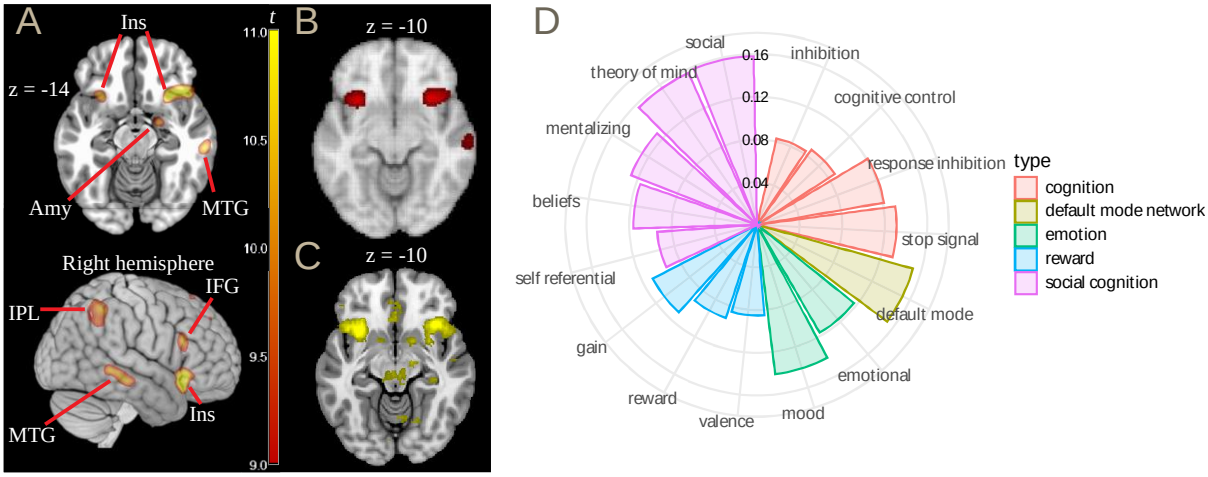

Figure 4. A: contrast time on task × high vs low reward: areas active at high threshold levels (*t* > 9.0). B: connectivity map of ACC seed, showing high co-activation in anterior insula. C: meta-analytic co-activation map (*z* > 4.0), showing co-activation in anterior insula and central nucleus of the amygdala. D: decoding analysis of this contrast (from www.neurosynth.org). ACC = anterior cingulate cortex; Amy = amygdala; IFG = inferior frontal gyrus; Ins = insula; IPL = inferior parietal lobule; MTG = middle temporal gyrus.

Subcortically, similarly to the result in the time on task contrast, activations were detected in the NBM/Ch4 (peaking bilaterally in x, y, z: 21, -4, -11, $t = 9.19$, and -19, -1, -13, $t = 6.40$, all $p < 0.001$, here and in the following voxel-level corrected at smoothing 4mm), also including the centromedial amygdaloid nucleus (x, y, z: 21, -4, -13, $t = 9.24$, $p < 0.001$, and -19, -2, -14, $t = 5.29$, $p = 0.015$). Differently from the activations found in the time on task contrast, these regions included both lateral and medial components of the Ch4 and presented a more specific localization. Also VTA/SN was involved, showing a small but significant effect (x, y, z: 3, -14, -13, $t = 5.15$, $p = 0.025$), and the thalamus (x, y, z: 9, -1, 6, $t = 6.96$, $p < 0.001$). There was no significant interaction between time on task and reward levels in the NAcc and in the locus coeruleus (x, y, z: 4, -36, -19, $t = 2.00$, $p > 0.05$, all voxel-level corrected at smoothing 4mm).

In summary, the interaction between time on task and reward revealed that at high reward levels both increases and decreases of cortical activity associated with the time on task were essentially a more lateralized subset of those of the time on task effect. In the basal forebrain, the involvement of areas consistent with recruitment of the Ch4 component of NBM was more specific than in the main effect. In the midbrain, the VTA exhibited a small but significant sensitivity to higher levels of reward.

Discussion

Four neural substrates were implicated in our hypotheses about the processes recruited by time on task. The first were frontal cortical substrates, implicated by psychological models as well as in previous neuroimaging empirical and theoretical literature (Langner & Eickhoff, 2013; Shenhav et al., 2013; Shenhav et al., 2016; Shenhav et al., 2017). The second was noradrenergic activity from the locus coeruleus, which is present as a modulator of cortical activity in several models. Third were the substrates of the reward system, implicated by the evidence on the energizing effects of reward and models of opportunity costs to explain diminishing attentional effects (Botvinick & Braver, 2015). Finally, numerous animal studies have provided evidence of cholinergic BF activity in the presence of cognitive challenges of various natures, including time on task (Sarter et al., 2006).

Cortical effects of time on task and its interaction with reward levels

The strong and distributed cortical evidence found in the present study, with a predominance of right-lateralized prefrontal and parietal areas, has been widely associated with sustained attention and cognitive control in the literature (Coull, 1998; Norman & Shallice, 1986; Robertson & O'Connell, 2010; Shallice & Burgess, 1996). These areas, summarized by the meta-analysis on sustained attention conducted by Langner and Eickhoff (2013), included the superior frontal gyrus, ACC, and the insula/inferior frontal gyrus. The functional involvement of thalamus, also present here, is frequently reported in sustained attention literature (Coull, 1998; Langner & Eickhoff, 2013; Riccio et al., 2002), and is considered to play a role in regulating the arousal state (Paus, 2000; Paus et al., 1997).

Similitudes aside, there were also differences between our results and those of previous studies, as summarized by Langner and Eickhoff (2013). The areas recruited by time on task were embedded in a much more extensive modulation of cortical activity. Instead of presenting as discrete specific areas, the effects of time on task may be better described as gradients of activation peaking in anterior and posterior cingulate cortex, the anterior insula, and the frontal and superior parietal foci.

Because of the empirical evidence of the effect of reward on cognitive effort (Botvinick & Braver, 2015), it is the interaction between time on task and reward levels that may throw light on the substrates specifically involved in modulation of control. We found that the areas most involved with time on task were also modulated by reward levels, supporting their role as the neural correlates of the energization of attentional processes by reward (Botvinick & Braver, 2015; Dutra et al., 2018; Esterman et al., 2017; Esterman et al., 2014; Massar et al., 2016; Tomporowski & Tinsley, 1996). Among these areas, the ACC and the right anterior insula stood out by presenting the largest effects. Comparison with rest connectivity data revealed these areas to form a highly connected network, which may constitute the core of the neural mechanism for the modulation of control in association with reward levels.

This finding is consistent with the notion that ACC computes signals tracking the cognitive control demands required to maximize the difference between expected benefits and intrinsic costs of cognitive efforts (Shenhav et al., 2013; Shenhav et al., 2016; Shenhav et al., 2017). The same model attributes to the anterior insula the role of providing input to the ACC about salient events in the environment requiring control adjustment, and the involvement of the lateral prefrontal cortex, also active here, in the implementation of the control process specified by the ACC (Shenhav et al., 2013). However, there was no activity in the region of the locus coeruleus in any contrast in our data, as hypothesized by this model.

A novel finding was that there were also cortical areas where activity decreased with time on task. These were the motor, premotor, and sensory cortex (extending ventrally into the parietal operculum) and left visual association areas. These decrements were more marked in high reward trials, arguing for their functional nature. In the neuroimaging literature, decreases in cortical activity have been interpreted as neural correlates of priming effects (Barron et al., 2016; Henson, 2003; Schacter & Buckner, 1998). Priming in neuroimaging studies has been shown to ensue from diverse mechanisms. Perceptual or neural priming is typically localized in associative visual or auditory areas (Grill-Spector et al., 2006; Wiggs & Martin, 1998). Priming may therefore explain the decrements in the left visual association areas observed here. Activity decrements in frontal areas have been attributed to conceptual priming (Race et al., 2009; Schacter et al., 2004), but the prefrontal areas described in these studies did not show decrements in our data.

In the present study, the largest activity decreases, located in the sensorimotor cortex, may not be consistent with perceptual priming, given the visual nature of the stimuli. However, decrements during time on task in the sensorimotor cortex may be observed for example in decision making (where participants decide between options presented on the right and the left with a button click, as was the case here) as part of a larger pattern of activity decreases that include visual associative cortex (Viviani, Dommes, Bosch, & Labek, 2020). Decreases in activity with time on task during passive exposure to visual stimuli similarly involve visual associative cortex, while sparing the sensorimotor areas (Labek & Viviani, 2025, in press). In the present study, the associative visual cortex was also involved, although to a lesser extent. We speculate that the very simple task of the present study may explain the regionally limited involvement of activity decreases in visual associated cortex, relative to what observed in a decision-making task with more complex stimuli, and the more marked involvement of sensorimotor areas.

Recruitment of VTA/SN and NAcc

We hypothesized that VTA/SN activity may decrease during the foraging patch and encode the diminished returns of the task at the net of the "opportunity cost" of rewards from alternative courses of action, or the increased cost of maintaining the task set. Contrary to our hypothesis, activity in VTA did not decrease during the forage patch, showing instead a modest but significant increase.

There are several possible reasons for the discrepancies between our result and previous observations of decreased activity in dopaminergic substrates representing outcomes discounted by effort (Botvinick et al., 2009; Kurniawan et al., 2013). First, the results in Botvinick et al. (2009) were obtained by looking at differences between obtained and expected outcomes (prediction errors), a signal that in our paradigm arises at the cue, not during the foraging patch. Indeed, the paradigm was designed to disentangle between motivation triggered by reward-predicting cues and the motivation to work to obtain expected rewards (Viviani, Dommes, Bosch, Steffens, et al., 2020). Second, the areas identified by Kurniawan et al. (2013) were in the ventral putamen and pallidum, and were more posterior than the NAcc. Our data did contain time on task activity decreases in the pallidum. However, it appeared to be located more posteriorly than the activity reported by these authors, making its interpretation uncertain.

The modulation of dopaminergic substrates we observed in the interaction between reward and ToT differed from those induced by levels of reward in the task, because it was limited to the VTA/SN and did not involve NAcc. In the ToT contrast, NAcc activity increased, but this increase was part of a general activity of the whole caudate. Our findings confirm the involvement of NAcc in the increased energization of responses in the high reward trials (Salamone & Correa, 2012), but not in the effects of reward on ToT activity. These findings are consistent with those from the animal literature, which suggest that the modulation of the dopaminergic system by expected effort requirements is weak and inconstant, in contrast to the modulation associated with prospective rewards (Walton & Bouret, 2019). Unlike NAcc, VTA/SN (together with NBM, see below) was sensitive to the progression of the foraging blocks at different reward levels, during which tracking the rewards accrued by the foraging activity represents a computation of possible relevance to remaining on task.

Recent data on laboratory animals have uncovered several populations of neurons in the VTA (Morales & Margolis, 2017), whose diverse functions are only beginning to be understood (Bouarab et al., 2019; Creed et al., 2014) but include tracking the value of expected reward that is required to compute changes in reward expectancies (prediction error, Eshel et al., 2015). Unlike dopamine neurons, a GABA subpopulation has been shown to fire irrespective of cues

signaling changes in reward expectancies, tracking the value of reward during the consummatory phase instead, and to project to pallidal neurons coding reward-dependent motor activity (Zhou et al., 2022). By observing the effect of stimulating this VTA-pallidal circuit, the authors show it to be instrumental in maintaining motivation to work for rewards. Furthermore, this activity is dissociable from the dopaminergic drive in NAcc (Brown et al., 2012). NAcc shell activity is inhibited by VTA GABA neurons (Al-Hasani et al., 2021), resulting in increased place preference and operant responding (Al-Hasani et al., 2021). While our understanding of VTA is still too incomplete to draw conclusions on the interpretation of our findings, we believe that there are considerable points of contacts between the characteristics of the VTA-pallidal GABAergic circuits of the animal literature and the VTA activity uncovered here and in a previous neuroimaging study (Viviani, Dommes, Bosch, Steffens, et al., 2020).

Recruitment of putative cholinergic substrates in the basal forebrain

The involvement of cholinergic BF in cognition is supported by the abundant evidence in sustained attention paradigms in animal studies (Gritton et al., 2016; Harati et al., 2008; Liu et al., 2018; Martinez & Sarter, 2004; McGaughy et al., 2002; McGaughy et al., 1999). In this literature, NBM cholinergic activity increases in the presence of “cognitive challenges”, i.e. factors that hinder the regular execution of the task, of which time on task is one example (Sarter et al., 2006). About 90% of the NBM consists of cholinergic neurons known as Ch4 (Koulousakis et al., 2019; Mesulam, 2013; Mesulam et al., 1983), which constitute the main source of cholinergic projections to the cortex (Mesulam et al., 1983).

In contrast to these animal studies, the recruitment of cholinergic components of BF has been rarely reported in sustained attention human studies (for an exception, see Howe et al., 2013). It should be emphasized that in our findings Ch4 recruitment became spatially specific only in the interaction between time on task and reward levels. The effects of time on task alone in Ch4, while not incompatible with its recruitment, were not conclusive due to the enmeshment of this region in a stronger regional pattern of activation.

Our findings are consistent with those of animal studies reporting the involvement of NBM when processing reward-related information, as in reward anticipation (Martinez-Rubio et al., 2018; Richardson & DeLong, 1986), reward/punishment delivery (Hangya et al., 2015; Richardson & DeLong, 1986), and cue-reward learning (Crouse et al., 2020). In a sustained attention paradigm in mice, Tashakori-Sabzevar and Ward (2018) demonstrated BF involvement in converting the motivational importance of probability signals of reward into enhanced attentional performance. As argued by Sarter et al. (2006), cholinergic BF may play a role in the modulation of increases in attentional effort, in particular in the presence of cognitive challenges and when motivated by a rewarding outcome. In this literature, cholinergic activity is often considered as supporting cognition in the face of challenging conditions, a compensatory mechanism distinct from motivation. Our data support the distinction between mechanisms involved in motivation and those involved in sustaining effort related to rewards, as NAcc was not recruited in the interaction between time on task and reward levels, in contrast to VTA/SN and NBM.

Our finding of the selective involvement of NBM/Ch4 in the interaction with reward levels may open the way to the use of this neuroimaging phenotype in future studies of individual differences (Wolpe et al., 2024), for example in the study of aging.

Conclusion

The cortical effects of time on task confirmed the results of previous studies of cognitive effort and sustained attention and showed that varying levels of reward may modulate these effects consistently with the facilitatory effects of reward on cognitive effort. However, our effects also included areas where activity decreased with time on task, such as the premotor/motor and somatosensory cortex, and involved most of the cortical mantle. We found no evidence of involvement of the locus coeruleus in any of the contrasts we examined.

We found no evidence in support of our initial hypothesis that dopaminergic substrates may signal diminishing levels of perceived returns, after discounting increasing effort while remaining on task. Instead, time on task was associated with increasing NBM/Ch4 activity, which was consistent with the abundant evidence for the involvement of this nucleus in the animal literature. This activity was best identified in the modulation of time on task by reward, together with activity in VTA/SN.

This finding suggests a partial dissociation of dopaminergic and cholinergic activity in the modulation of cognitive control. NAcc, which is widely associated with the motivational effects of reward and was here more active in high reward trials, was not involved in the modulation of the time on task by reward levels. In contrast, this modulation was associated with NBM/Ch4 and VTA/SN activity, which may identify a distinct phenotype involved in the maintenance of task sets and cognitive effort in interaction with a cortical network centered on ACC and the anterior insula.

Materials and methods

Participants

The data used in the present study were collected as part of a genetic imaging research project (Viviani, Messina, et al., 2020). After obtaining written informed consent, 441 healthy participants were screened for psychiatric disorders, and they were excluded if they presented current substance (alcohol or drug) addiction, anorexia, present affective disorders, pregnancy or breastfeeding, severe acute or chronic illness, assumption of psychoactive or long-term medications, presence of metal implants, large tattoos, or tattoos near the head. Further exclusion criteria in later stages of the study (imaging scan or data analysis) were the presence of clinical findings, artifacts or excessive movements, and equipment or task administration/completion failures. The final sample consisted of 415 subjects (234 females, age range 18-45, mean age 23.43 ± 3.80 years). Data of 58 participants were collected at the German Center for Neurodegenerative Diseases (DZNE) in Bonn, the one of 357 were collected at the University of Ulm.

The study (acronym: BrainCYP) was registered in the German Clinical Trials Register (DRKS-ID: 00011722), followed the guidelines of the Declaration of Helsinki, and was approved by the Ethical Committee of the University of Bonn (No. 33/15) and the Ethical Committee of the University of Ulm (No. 01/15).

Experimental paradigm

The paradigm used here (Figure 1A) was introduced in previous studies (Viviani, Dommes, Bosch, Steffens, et al., 2020; Viviani, Messina, et al., 2020). While inside the MRI scanner, participants executed a sustained attention paradigm consisting of 16 blocks, which were characterized by two possible rewarding levels: high and low. Each block consisted of the 2s presentation of a cue, providing information on the reward level, a 3s fixation cross, and a

“foraging patch”, lasting approximately 15s, started. During the foraging patch, participants had 0.8s to press a button congruently with the location of a dot appearing in the left or right side of the fixation cross (i.e., left button in case of left-presented dot; right button in case of right-presented dot). The interstimulus interval (ISI) varied according to a Poisson schedule with an average temporal interval of 1.23s. Between the end of one block and the beginning of another, a fixation cross was presented for 10s. Participants collected virtual coins when responding correctly (20 cents per correct response in the high reward blocks, 1 cent in the low reward blocks). The final monetary reward was obtained only if participants had won a total minimum amount of 20 euros. Participants were informed that they would need to provide correct and rapid answers during both the high and low reward trials to reach that threshold. The whole duration of the task was equal to 8 minutes. Participants had the opportunity to practice the task prior to being positioned in the scanner.

fMRI data acquisition

Neuroimaging data were collected at the German Center for Neurodegenerative Diseases (DZNE) in Bonn and at the Department of Psychiatry and Psychotherapy of the University of Ulm, using respectively a 3 T Siemens Skyra scanner, and a 3 T Siemens Prisma scanner. 64-channels head coils were used, and a T2*-weighted echo-planar imaging sequence was applied (TR/TE of 2460/30 ms; flip angle of 82°; FOV measuring 24 cm; matrix size of 64 × 64 pixels with dimension of 3 × 3 mm in 39 transversal slices, each 2.5 mm thick, and acquired in ascending order with a gap between slices set at 0.5 mm for an isotropic pixel size of 3 mm). Since regions with high susceptibility or areas presenting high iron levels have a shorter T2*, a compensation was performed by progressively reducing the TE by 8 ms from slice 24 to slice 14. This resulted in a TE of 22 ms for the initial 14 slices acquired in the bottom of the volume (see the procedure in Stöcker et al., 2006). T1-weighted structural images were collected and assessed individually to detect eventual abnormalities.

Masks of subcortical areas

The cholinergic Ch4 NBM component was identified with the JuBrain Anatomy toolbox by Eickhoff et al. (2006); Eickhoff et al. (2007); Eickhoff et al. (2005); Zaborszky et al. (2008). The JuBrain Anatomy toolbox was used also for the identification of amygdalar structures (Amunts et al., 2005; Eickhoff et al., 2006; Eickhoff et al., 2007; Eickhoff et al., 2005; Kedo et al., 2018). VTA/SN were identified using the probabilistic maps by Ballard et al. (2011); Murty et al. (2014). The NAcc was identified using the Harvard Oxford Atlas (Desikan et al., 2006; Frazier et al., 2005; Goldstein et al., 2007; Makris et al., 2006) distributed by FMRIB Software Library https://fsl.fmrib.ox.ac.uk/. The locus coeruleus was identified using the two standard-deviations-mask by Keren et al. (2009).

Data analysis

Neuroimaging analyses were carried out using the freely available software SPM12 (Wellcome Trust Centre for Neuroimaging, http://www.fil.ion.ucl.ac.uk/spm/) running on MATLAB (The MathWorks, https://www.mathworks.com). After realignment, data were registered to standard Montreal Neurological Institute (MNI) space. In the segmentation step, the spatial priors provided by this software were supplemented with a prior comprising the pallidum, red nucleus, and substantia nigra (as in Viviani, Dommes, et al., 2020). After registration to MNI space and resampling to a voxel size of 1.5 mm, two separate datasets were obtained by smoothing the data with Gaussian kernels of 8 and 4 mm FWHM. In the analyses, the 8 mm smoothing dataset was used for cortex (reported in the tables in the Appendix) and the 4 mm for subcortical nuclei and the amygdala (reported in main text).

At the first level, the task was modeled by four groups of zero-duration onset series, two for the cue events (low and high reward) and two for the trials (the presentations of the individual targets) in the forage patches (low and high reward). The onsets were then convolved with the canonical hemodynamic response function. Time on task was modeled as a parametric modulator given by the number of the trial within the forage patch, after centering. As a result, estimates of the foraging effects refer to activity in the middle of the foraging patch, and the parametric modulator coefficient measures the increase of activity during the patch. Centering the time on task predictor also ensured that all model predictors were reciprocally orthogonal, splitting the variance of the signal into uncorrelated components. Confounding covariates were the mean signals of white matter, ventricles, and cranial bone (Huber et al., 2024) as separate regressors, the six head movement terms estimated at the realignment step and their second derivatives (12 movement parameters in all).

Contrasts of interest in previous analyses of this paradigm assessed the effect of reward levels at the presentation of the cue and during the forage patch (high vs. low reward). Here, the contrasts of interest concerned the parametric modulators: the increase in activity during the foraging patch, and the differences in these increases between the conditions of high and low reward levels. Contrast images were taken to the second level and tested by permutation (8000 resamples, cluster-defining threshold $p = 0.001$, uncorrected). Contrasts from the 8 mm smoothing dataset were used for the primary analysis of cortical effects in Figures and in the Tables in the Appendix. Contrasts from the 4 mm smoothing dataset were reported in the main text and were used to assess effects in locus coeruleus, thalamus, NBM/Ch4, amygdalae, VTA/SN, and NAcc, identified by masks as described in the section “Mask of subcortical areas”. The freely available software MRICroN (Chris Rorden, https://people.cas.sc.edu/rorden/mricron) was used to visualize parametric maps.

The decoding analysis was conducted with the “Neurosynth Image Decoder” function in the neurosynth database (www.neurosynth.org). This function loads the whole-brain parametric map of *t* values arising from a contrast of interest and compares the overall spatial distribution of the statistics with that of the other parametric maps of the database. The maps contain keywords referring to the original contrast of interest, allowing a meta-analytic automatic comparison of the activity pattern with the patterns of the images in the database.

Analyses of RTs, accuracy, and plots were generated using the freely available software R version 4.4.0 (R: The R Project for Statistical Computing, r-project.org) using the packages dplyr (Wickham, François, et al., 2023), tidyr (Wickham, Vaughan, et al., 2023), lme4 (Bates et al., 2015), and ggplot2 (Wickham, 2016). After excluding missed trials, RTs were filtered using a threshold between 0.25s and 0.8s. The model was fitted with the function *lmer* and included trial number within the block (time on task), first trial indicator, reward level, block number, ISI, side switch of target relative to previous trial, acquisition site, and an individual group variable modelled as a random effect (see the Supplementary Materials section for robustness analyses R code). Accuracy analysis was carried out with a logistic regression (function *glmer*) replicating, in terms of predictors, the structure of reaction times model. Here, correct hits were coded as success, and incorrect responses and misses were coded as failures in the logistic regression.

Acknowledgements

A preliminary version of this work was presented at the CogBases workshop (Paris, Institut Pasteur, 10-11 October 2023). This work was supported by an ERA-PERMED grant (project ArtiPro) of the FWF Austrian Science Fund (grant number I 5903) [Grant-DOI: 10.55776/I5903] to Roberto Viviani. The authors declare no conflict of interest.

Appendix

Table A1. Forage trend. Effect of time on task, positive direction.

Clu #	Brain area	Coord. (mm.)	*t*	*p* (uncorr.)	*p* (corr.)	*k*	*p* (cl.)
1	R Posterior Cingulate Gyrus (BA 23)	9 -40 41	22.046	< 0.0001	<0.001	291531	<0.001
	R Superior Frontal Gyrus (BA 9)	25 35 38	20.598	< 0.0001	<0.001		
	L Anterior Cingulate (BA 11)	-7 33 0	20.238	< 0.0001	<0.001		
	R Inferior Frontal Gyrus (BA 47)	28 23 -7	20.143	< 0.0001	<0.001		
	R Superior Temporal Gyrus (BA 41)	54 -20 5	19.707	< 0.0001	<0.001		
	R Superior Frontal Gyrus (BA 8)	27 23 54	19.699	< 0.0001	<0.001		
	R Lentiform Nucleus (Putamen)	31 -19 -1	19.387	< 0.0001	<0.001		
	R Precuneus (BA 31)	9 -64 23	19.366	< 0.0001	<0.001		
	R Inferior Frontal Gyrus (BA 47)	30 29 -16	19.350	< 0.0001	<0.001		
	R Anterior Cingulate (BA 32)	9 33 21	19.335	< 0.0001	<0.001		
	L Insula (BA 13)	-28 18 -7	19.318	< 0.0001	<0.001		
	R Anterior Cingulate (BA 32)	4 36 27	19.103	< 0.0001	<0.001		
	R Medial Frontal Gyrus (BA 8)	4 26 44	19.102	< 0.0001	<0.001		
	R Lingual Gyrus (BA 18)	22 -88 -5	18.690	< 0.0001	<0.001		
	R Anterior Cingulate (BA 11)	9 38 5	18.630	< 0.0001	<0.001		
	R Precentral Gyrus (BA 6)	39 -11 35	18.496	< 0.0001	<0.001		
	R Precuneus (BA 39)	42 -70 35	18.297	< 0.0001	<0.001		
	L Caudate (Caudate Head)	-12 15 2	18.265	< 0.0001	<0.001		
	L Superior Temporal Gyrus (BA 41)	-45 -26 3	18.238	< 0.0001	<0.001		
	L Precentral Gyrus (BA 4)	-37 -14 35	18.096	< 0.0001	<0.001		
	R Inferior Parietal Lobule (BA 39)	37 -62 42	17.711	< 0.0001	<0.001		
	R Middle Frontal Gyrus (BA 9)	46 27 26	17.627	< 0.0001	<0.001		
	R Cuneus (BA 18)	10 -79 23	17.472	< 0.0001	<0.001		
	L Medial Frontal Gyrus (BA 4)	-6 -26 63	17.419	< 0.0001	<0.001		
	R Inferior Frontal Gyrus, Orbital Part (BA 47)	40 33 -17	17.381	< 0.0001	<0.001		
	L Medial Frontal Gyrus (BA 9)	-24 36 33	17.342	< 0.0001	<0.001		
	R Middle Frontal Gyrus (BA 46)	48 32 18	17.231	< 0.0001	<0.001		
	L Precuneus (BA 23)	-7 -67 23	17.197	< 0.0001	<0.001		
	R Medial Frontal Gyrus (BA 4)	6 -22 65	17.148	< 0.0001	<0.001		

R Precuneus (BA 7)	13 -77 33	17.077	< 0.0001	<0.001
L Cingulate Gyrus (BA 31)	-6 -38 41	17.057	< 0.0001	<0.001
L Inferior Frontal Gyrus (BA 47)	-28 24 -14	16.921	< 0.0001	<0.001
L Angular Gyrus (BA 39)	-40 -77 32	16.814	< 0.0001	<0.001
R Middle Temporal Gyrus (BA 21)	60 -46 2	16.798	< 0.0001	<0.001
R Inferior Frontal Gyrus (BA 38)	43 27 -13	16.781	< 0.0001	<0.001
L Middle Frontal Gyrus (BA 8)	-24 14 51	16.678	< 0.0001	<0.001
R Middle Frontal Gyrus (BA 44)	39 12 42	16.512	< 0.0001	<0.001
L Superior Frontal Gyrus (BA 8)	-25 17 57	16.319	< 0.0001	<0.001
R Caudate	16 -2 18	15.901	< 0.0001	<0.001
R Lentiform Nucleus (Putamen)	28 0 -7	15.843	< 0.0001	<0.001
R Superior Temporal Gyrus (BA 22)	52 -49 20	15.461	< 0.0001	<0.001
L Precuneus (BA 19)	-36 -74 39	15.391	< 0.0001	<0.001
R Superior Frontal Gyrus (BA 10)	25 54 8	15.332	< 0.0001	<0.001
R Medial Frontal Gyrus (BA 11)	7 48 -13	15.210	< 0.0001	<0.001
R Caudate (Caudate Head)	10 14 5	15.159	< 0.0001	<0.001
L Inferior Parietal Lobule (BA 7)	-31 -61 41	15.159	< 0.0001	<0.001
R Medial Frontal Gyrus (BA 10)	6 47 -10	15.139	< 0.0001	<0.001
R Cuneus (BA 18)	7 -68 3	15.053	< 0.0001	<0.001
L Inferior Frontal Gyrus, Orbital Part (BA 47)	-43 32 -19	14.968	< 0.0001	<0.001
L Superior Temporal Gyrus (BA 22)	-58 -29 5	14.829	< 0.0001	<0.001
L Middle Frontal Gyrus (BA 46)	-48 20 24	14.761	< 0.0001	<0.001
L Superior Frontal Gyrus (BA 10)	-22 53 11	14.538	< 0.0001	<0.001
L Middle Temporal Gyrus (BA 21)	-63 -49 5	14.500	< 0.0001	<0.001
R Middle Temporal Gyrus (BA 21)	48 -28 -7	14.400	< 0.0001	<0.001
R Anterior Prefrontal Cortex (BA 46)	25 45 17	14.391	< 0.0001	<0.001
R Superior Frontal Gyrus, Orbital Part (BA 11)	19 54 -7	14.163	< 0.0001	<0.001
L Precuneus (BA 7)	-6 -65 45	14.132	< 0.0001	<0.001
L Cuneus (BA 18)	-6 -80 23	14.005	< 0.0001	<0.001
R Middle Temporal Gyrus (BA 20)	49 -19 -13	13.992	< 0.0001	<0.001
R Parahippocampal Gyrus (BA 28)	21 -13 -22	13.989	< 0.0001	<0.001
L Middle Frontal Gyrus (BA 44)	-43 14 32	13.954	< 0.0001	<0.001
R Middle Temporal Gyrus (BA 21)	58 -19 -13	13.930	< 0.0001	<0.001
R Superior Frontal Gyrus (BA 11)	22 51 -1	13.661	< 0.0001	<0.001
R Lingual Gyrus (BA 18)	16 -70 -4	13.657	< 0.0001	<0.001
R Inferior Parietal Lobule (BA 40)	48 -43 50	13.502	< 0.0001	<0.001
L Supramarginal Gyrus (BA 22)	-60 -52 21	13.066	< 0.0001	<0.001

L Parahippocampal Gyrus (BA 28)	-21 -14 -22	12.959	< 0.0001	<0.001
R Parahippocampal Gyrus (BA 19)	19 -46 -7	12.887	< 0.0001	<0.001
L Thalamus	-6 -7 -1	12.658	< 0.0001	<0.001
L Cingulate Gyrus	-7 -20 29	12.569	< 0.0001	<0.001
R Postcentral Gyrus (BA 2)	61 -23 36	12.221	< 0.0001	<0.001
R Thalamus	6 -8 2	12.046	< 0.0001	<0.001
R Middle Frontal Gyrus (BA 10)	43 54 -13	11.924	< 0.0001	<0.001
L Middle Frontal Gyrus (BA 47)	-34 36 -1	11.918	< 0.0001	<0.001
L Middle Temporal Gyrus (BA 20)	-51 -14 -14	11.885	< 0.0001	<0.001
R Postcentral Gyrus (BA 1)	58 -28 44	11.874	< 0.0001	<0.001
R Superior Frontal Gyrus (BA 11)	31 54 -17	11.601	< 0.0001	<0.001
L Fusiform Gyrus (BA 20)	-55 -16 -31	11.450	< 0.0001	<0.001
R Superior Frontal Gyrus (BA 11)	33 60 -4	11.226	< 0.0001	<0.001
R Parahippocampal Gyrus (BA 37)	31 -40 -13	11.002	< 0.0001	<0.001
R Inferior Temporal Gyrus (BA 20)	52 -28 -25	10.657	< 0.0001	<0.001
L Lentiform Nucleus (Putamen)	-31 -20 -2	10.653	< 0.0001	<0.001
R Fusiform Gyrus (BA 20)	43 -17 -31	10.632	< 0.0001	<0.001
R Anterior Cingulate (BA 24)	1 -2 29	10.575	< 0.0001	<0.001
L Hippocampus (BA 20)	-28 -8 -13	10.545	< 0.0001	<0.001
L Fusiform Gyrus (BA 20)	-45 -19 -28	10.304	< 0.0001	<0.001
L Inferior Temporal Gyrus (BA 20)	-57 -4 -34	10.150	< 0.0001	<0.001
R Thalamus (Medial Dorsal Nucleus)	6 -20 2	10.077	< 0.0001	<0.001
R Parahippocampal Gyrus (BA 20)	30 -25 -17	10.010	< 0.0001	<0.001
R Thalamus	7 -22 0	9.968	< 0.0001	<0.001
R Parahippocampal Gyrus (BA 20)	31 -28 -16	9.964	< 0.0001	<0.001
R Fusiform Gyrus (BA 20)	40 -28 -23	9.852	< 0.0001	<0.001
L Parahippocampal Gyrus (BA 36)	-30 -37 -13	9.798	< 0.0001	<0.001
L Fusiform Gyrus (BA 20)	-45 -31 -25	9.752	< 0.0001	<0.001
L Inferior Temporal Gyrus (BA 20)	-60 -34 -25	9.746	< 0.0001	<0.001
R Inferior Temporal Gyrus (BA 20)	54 0 -38	9.536	< 0.0001	<0.001
L Cingulate Gyrus (BA 24)	-10 -10 41	9.260	< 0.0001	<0.001
L Middle Frontal Gyrus, Orbital Part (BA 10)	-37 57 -14	8.976	< 0.0001	<0.001
R Cingulate Gyrus (BA 24)	9 -10 41	8.533	< 0.0001	<0.001
L Lingual Gyrus (BA 27)	-18 -44 -4	8.450	< 0.0001	<0.001
L Superior Frontal Gyrus (BA 11)	-30 50 -19	8.185	< 0.0001	<0.001
L Superior Temporal Gyrus (BA 38)	-40 14 -26	8.122	< 0.0001	<0.001
R Insula (BA 13)	36 -14 18	8.057	< 0.0001	<0.001
L Supramarginal Gyrus (BA 40)	-64 -34 39	7.017	< 0.0001	<0.001

	L Brainstem (Midbrain)	0 -20 -19	6.736	< 0.0001	<0.001		
	L Culmen (BA 30)	-6 -43 -10	5.561	< 0.0001	0.001		
	R Middle Temporal Gyrus (BA 20)	36 2 -50	4.953	< 0.0001	0.010		
2	L Lingual Gyrus (BA 18)	-19 -89 -7	10.965	< 0.0001	<0.001	1370	0.018
3	L Declive	-15 -74 -28	7.152	< 0.0001	<0.001	1764	0.011
	L Uvula	-27 -65 -31	7.116	< 0.0001	<0.001		
4	R Nodule	9 -47 -37	5.516	< 0.0001	0.001	253	0.214

Peaks with significance p = 0.001 or less, uncorrected. Peaks at minimum distance 10 mm. Clu#: cluster number; Coord. (mm.): coordinates in Montreal Neurological Institute; p (uncorr.): significance value, uncorrected; p (corr.): significance value, peak-level corrected; k: cluster extent (in 1.5 mm voxels); p (cl.): significance value, cluster-level corrected.

Table A2. Forage trend. Effect of time on task, negative direction.

Clu #	Brain area	Coord. (mm.)	t	p (uncorr.)	p (corr.)	k	p (cl.)
1	L Precentral Gyrus (BA 6)	-40 -14 56	-31.364	< 0.0001	<0.001	96263	<0.001
	L Postcentral Gyrus (BA 1)	-52 -19 48	-26.835	< 0.0001	<0.001		
	R Culmen (BA 37)	22 -52 -22	-23.574	< 0.0001	<0.001		
	L Rolandic Operculum	-48 -22 20	-21.693	< 0.0001	<0.001		
	R Precentral Gyrus (BA 6)	40 -13 53	-20.990	< 0.0001	<0.001		
	L Medial Frontal Gyrus (BA 6)	-6 -2 57	-19.793	< 0.0001	<0.001		
	L Insula (BA 6)	-42 -2 15	-18.840	< 0.0001	<0.001		
	L Middle Temporal Gyrus (BA 19)	-43 -74 6	-18.606	< 0.0001	<0.001		
	L Inferior Frontal Gyrus (BA 9)	-60 6 32	-15.103	< 0.0001	<0.001		
	L Middle Occipital Gyrus (BA 19)	-34 -74 -14	-14.232	< 0.0001	<0.001		
	R Precentral Gyrus (BA 6)	36 -23 68	-14.128	< 0.0001	<0.001		
	L Superior Parietal Lobule (BA 7)	-27 -52 68	-13.648	< 0.0001	<0.001		
	R Culmen (BA 18)	7 -59 -14	-12.130	< 0.0001	<0.001		
	L Precuneus	-6 -58 72	-12.099	< 0.0001	<0.001		
	R Insula	40 -1 17	-11.940	< 0.0001	<0.001		
	L Precuneus	-3 -52 74	-11.409	< 0.0001	<0.001		
	L Culmen (BA 37)	-25 -53 -22	-11.248	< 0.0001	<0.001		
	R Lingual Gyrus	7 -94 -19	-10.950	< 0.0001	<0.001		
	R Cuneus (BA 17)	1 -100 -5	-10.803	< 0.0001	<0.001		
	R Tuber	52 -52 -34	-10.668	< 0.0001	<0.001		
	L Declive	-51 -59 -28	-10.603	< 0.0001	<0.001		
	L Calcarine (BA 17)	-1 -103 0	-10.309	< 0.0001	<0.001		
	R Cerebellar Crus I	36 -85 -25	-10.192	< 0.0001	<0.001		
	L Precuneus	-3 -47 75	-10.124	< 0.0001	<0.001		
	R Fusiform Gyrus (BA 18)	24 -91 -23	-10.063	< 0.0001	<0.001		

	R Declive	48 -59 -29	-9.845	< 0.0001	<0.001		
	L Paracentral Lobule	-1 -40 78	-9.755	< 0.0001	<0.001		
	L Uvula (BA 18)	-12 -92 -23	-9.668	< 0.0001	<0.001		
	R Precuneus (BA 5)	1 -44 75	-9.417	< 0.0001	<0.001		
	L Precuneus (BA 5)	-7 -50 78	-9.366	< 0.0001	<0.001		
	R Pyramis	3 -65 -34	-9.332	< 0.0001	<0.001		
	L Cuneus (BA 19)	-21 -91 18	-9.311	< 0.0001	<0.001		
	L Caudate	-18 5 26	-8.884	< 0.0001	<0.001		
	L Paracentral Lobule	-3 -32 80	-8.640	< 0.0001	<0.001		
	R Caudate	19 14 21	-8.559	< 0.0001	<0.001		
	R Superior Parietal Lobule (BA 7)	16 -67 68	-8.199	< 0.0001	<0.001		
	R Cuneus (BA 18)	6 -98 12	-8.167	< 0.0001	<0.001		
	R Superior Parietal Lobule (BA 7)	19 -58 62	-7.294	< 0.0001	<0.001		
	R Paracentral Lobule (BA 5)	4 -43 78	-6.981	< 0.0001	<0.001		
	R Supramarginal Gyrus (BA 1)	27 -38 45	-6.663	< 0.0001	<0.001		
	R Postcentral Gyrus	54 -16 20	-6.550	< 0.0001	<0.001		
	R Cingulate Gyrus	19 -1 29	-6.544	< 0.0001	<0.001		
	R Primary Sensory (BA 1)	25 -40 44	-6.506	< 0.0001	<0.001		
	L Precuneus	-1 -79 51	-6.487	< 0.0001	<0.001		
	R Inferior Frontal Gyrus (BA 9)	63 9 29	-6.440	< 0.0001	<0.001		
	L Cingulate Gyrus (BA 6)	-12 -22 45	-6.424	< 0.0001	<0.001		
	L Paracentral Lobule	-1 -22 80	-6.272	< 0.0001	<0.001		
	R Precuneus (BA 5)	6 -46 78	-5.940	< 0.0001	<0.001		
	R Insula	45 -20 21	-5.475	< 0.0001	0.001		
	R Hippocampus (BA 20)	39 -19 -16	-5.472	< 0.0001	0.001		
	R Rolandic Operculum	42 -22 23	-5.422	< 0.0001	0.001		
	L Precuneus (BA 7)	-6 -79 54	-4.499	< 0.0001	0.067		
	L Insula (BA 13)	-37 -5 0	-4.049	< 0.0001	0.270		
2	L Lentiform Nucleus (Medial Globus Pallidus)	-18 -7 -5	-11.080	< 0.0001	<0.001	4582	0.003
	R Hypothalamus (BA 25)	6 0 -14	-9.791	< 0.0001	<0.001		
	R Middle Temporal Pole (BA 36)	22 12 -34	-7.914	< 0.0001	<0.001		
	L Superior Temporal Gyrus (BA 38)	-24 12 -37	-6.947	< 0.0001	<0.001		
	R Lentiform Nucleus (Medial Globus Pallidus)	18 -5 -5	-6.887	< 0.0001	<0.001		
	L Superior Temporal Gyrus (BA 38)	-28 18 -34	-5.899	< 0.0001	<0.001		
	L Orbital Gyrus (BA 11)	-16 36 -26	-5.309	< 0.0001	0.002		
	L Superior Temporal Gyrus (BA 38)	-31 20 -32	-4.945	< 0.0001	0.012		
	R Superior Temporal Gyrus (BA 38)	28 18 -32	-3.903	< 0.0001	0.391		
	L Inferior Frontal Gyrus (BA 11)	-22 29 -25	-3.869	< 0.0001	0.427		

	R Superior Temporal Gyrus (BA 38)	31 20 -34	-3.750	0.0001	0.538		
3	L Rectus (BA 11)	-3 66 -16	-8.721	< 0.0001	<0.001	940	0.033
	R Superior Frontal Gyrus, Orbital Part (BA 11)	10 68 -16	-6.609	< 0.0001	<0.001		
4	R Orbital Gyrus (BA 11)	16 35 -28	-6.924	< 0.0001	<0.001	90	0.526
5	L Middle Frontal Gyrus (BA 9)	-40 48 32	-5.267	< 0.0001	0.003	215	0.255
	L Middle Frontal Gyrus (BA 45)	-46 48 21	-3.398	0.0004	0.856		
6	L Superior Temporal Gyrus (BA 38)	-52 18 -22	-5.161	< 0.0001	0.004	19	0.870
7	L Substantia Nigra	-10 -20 -11	-5.111	< 0.0001	0.006	197	0.281

Peaks with significance p = 0.001 or less, uncorrected. Peaks at minimum distance 10 mm. Clu#: cluster number; Coord. (mm.): coordinates in Montreal Neurological Institute; p (uncorr.): significance value, uncorrected; p (corr.): significance value, peak-level corrected; k: cluster extent (in 1.5 mm voxels); p (cl.): significance value, cluster-level corrected.

Table A3. Forage trend high vs low. Interaction between time on task and reward, positive direction.

Clu #	Brain area	Coord. (mm.)	t	p (uncorr.)	p (corr.)	k	p (cl.)
1	R Medial Frontal Gyrus (BA 32)	4 41 23	14.041	< 0.0001	<0.001	155061	<0.001
	R Insula (BA 47)	30 21 -8	12.780	< 0.0001	<0.001		
	R Inferior Frontal Gyrus (BA 38)	45 21 -13	12.690	< 0.0001	<0.001		
	R Anterior Cingulate (BA 32)	7 42 5	12.191	< 0.0001	<0.001		
	R Inferior Frontal Gyrus (BA 47)	28 18 -13	12.175	< 0.0001	<0.001		
	R Lingual Gyrus (BA 18)	16 -71 -7	11.612	< 0.0001	<0.001		
	R Middle Temporal Gyrus (BA 21)	58 -40 -4	11.270	< 0.0001	<0.001		
	R Middle Temporal Gyrus (BA 20)	61 -26 -13	10.961	< 0.0001	<0.001		
	L Insula (BA 47)	-30 18 -16	10.839	< 0.0001	<0.001		
	R Medial Frontal Gyrus (BA 9)	9 41 42	10.768	< 0.0001	<0.001		
	R Parahippocampal Gyrus (Amygdala)	21 -4 -13	10.736	< 0.0001	<0.001		
	R Anterior Cingulate (BA 24)	4 27 18	10.576	< 0.0001	<0.001		
	R Inferior Parietal Lobule (BA 40)	49 -49 47	10.573	< 0.0001	<0.001		
	R Superior Frontal Gyrus (BA 6)	7 29 59	10.555	< 0.0001	<0.001		
	R Superior Frontal Gyrus (BA 10)	16 56 24	10.465	< 0.0001	<0.001		
	R Middle Temporal Gyrus (BA 21)	55 -28 -5	10.463	< 0.0001	<0.001		
	R Inferior Frontal Gyrus (BA 45)	52 23 23	10.462	< 0.0001	<0.001		
	R Superior Frontal Gyrus (BA 9)	13 48 36	10.298	< 0.0001	<0.001		
	L Declive	-27 -68 -28	9.669	< 0.0001	<0.001		
	R Middle Frontal Gyrus (BA 10)	24 62 9	9.272	< 0.0001	<0.001		
	R Precuneus (BA 19)	16 -83 38	9.144	< 0.0001	<0.001		
	R Middle Frontal Gyrus (BA 9)	43 12 50	9.011	< 0.0001	<0.001		

L Declive	-10 -80 -28	8.874	< 0.0001	<0.001
R Middle Frontal Gyrus (BA 47)	33 56 -1	8.804	< 0.0001	<0.001
R Middle Frontal Gyrus (BA 11)	45 44 -13	8.800	< 0.0001	<0.001
R Middle Frontal Gyrus (BA 47)	37 53 -5	8.688	< 0.0001	<0.001
R Cingulate Gyrus (BA 23)	1 -16 38	8.517	< 0.0001	<0.001
R Precentral Gyrus (BA 9)	46 20 39	8.423	< 0.0001	<0.001
R Posterior Cingulate (BA 30)	6 -62 5	8.286	< 0.0001	<0.001
R Caudate (Caudate Body)	13 8 14	8.238	< 0.0001	<0.001
R Hippocampus	21 -17 -11	8.187	< 0.0001	<0.001
R Thalamus	7 -5 8	7.992	< 0.0001	<0.001
R Precuneus (BA 7)	10 -79 47	7.858	< 0.0001	<0.001
R Cingulate Gyrus (BA 23)	7 -40 38	7.820	< 0.0001	<0.001
R Middle Frontal Gyrus (BA 46)	42 39 21	7.404	< 0.0001	<0.001
R Cuneus (BA 18)	6 -79 35	7.214	< 0.0001	<0.001
R Middle Temporal Gyrus (BA 37)	52 -58 -14	7.010	< 0.0001	<0.001
R Parahippocampal Gyrus (BA 27)	16 -40 -4	6.926	< 0.0001	<0.001
R Cuneus (BA 18)	7 -86 23	6.898	< 0.0001	<0.001
R Middle Temporal Gyrus (BA 37)	54 -53 -13	6.839	< 0.0001	<0.001
R Declive (BA 19)	31 -70 -26	6.809	< 0.0001	<0.001
R Parahippocampal Gyrus (BA 19)	19 -44 -7	6.707	< 0.0001	<0.001
L Superior Frontal Gyrus (BA 10)	-25 51 -2	6.582	< 0.0001	<0.001
L Inferior Frontal Gyrus (BA 47)	-51 36 -13	6.572	< 0.0001	<0.001
R Calcarine (BA 19)	22 -55 8	6.546	< 0.0001	<0.001
L Anterior Cingulate (BA 24)	-3 23 -5	6.530	< 0.0001	<0.001
L Inferior Frontal Gyrus (BA 45)	-58 20 12	6.529	< 0.0001	<0.001
L Lingual Gyrus (BA 18)	-6 -62 2	6.500	< 0.0001	<0.001
L Caudate (Caudate Head)	-9 6 0	6.469	< 0.0001	<0.001
L Tuber	-37 -76 -34	6.389	< 0.0001	<0.001
L Culmen (BA 37)	-18 -49 -19	6.334	< 0.0001	<0.001
R Lentiform Nucleus (Putamen)	18 9 -1	6.286	< 0.0001	<0.001
L Superior Frontal Gyrus (BA 8)	-10 27 56	6.232	< 0.0001	<0.001
L Culmen (BA 18)	-13 -55 -13	6.170	< 0.0001	<0.001
L Parahippocampal Gyrus (BA 34)	-18 -2 -13	6.121	< 0.0001	<0.001
R Inferior Temporal Gyrus (BA 37)	43 -49 -10	5.909	< 0.0001	<0.001
L Middle Frontal Gyrus (BA 47)	-34 54 -7	5.896	< 0.0001	<0.001
L Superior Frontal Gyrus (BA 9)	-19 44 32	5.841	< 0.0001	<0.001
R Superior Frontal Gyrus (BA 11)	16 54 -10	5.708	< 0.0001	0.001
L Posterior Cingulate (BA 17)	-21 -59 9	5.560	< 0.0001	0.001
L Cerebellar Tonsil	-7 -55 -41	5.530	< 0.0001	0.001

	L Superior Frontal Gyrus (BA 46)	-19 53 21	5.489	< 0.0001	0.002		
	R Brainstem (Midbrain)	7 -14 -11	5.386	< 0.0001	0.002		
	R Declive (BA 18)	12 -79 -23	5.304	< 0.0001	0.004		
	R Inferior Frontal Gyrus (BA 45)	36 29 11	5.139	< 0.0001	0.006		
	L Inferior Frontal Gyrus (BA 45)	-43 21 6	5.004	< 0.0001	0.012		
	L Uvula	-6 -70 -37	4.932	< 0.0001	0.016		
	R Parahippocampal Gyrus (BA 37)	28 -37 -13	4.755	< 0.0001	0.031		
	R Precuneus (BA 5)	3 -56 68	4.705	< 0.0001	0.036		
	L Posterior Cingulate (BA 30)	-15 -67 11	4.676	< 0.0001	0.041		
	L Lingual Gyrus (BA 19)	-15 -47 -5	4.607	< 0.0001	0.053		
	R Middle Temporal Gyrus (BA 20)	54 -7 -16	4.182	< 0.0001	0.228		
	L Cerebellar Tonsil	-36 -61 -44	4.155	< 0.0001	0.247		
	L Pyramis	-52 -65 -43	4.070	< 0.0001	0.317		
	R Thalamus	6 -26 0	3.760	< 0.0001	0.615		
	L Precentral Gyrus (BA 9)	-39 21 41	3.727	0.0001	0.650		
	L Cerebellar Tonsil	-19 -43 -47	3.670	0.0001	0.708		
	L Middle Frontal Gyrus (BA 9)	-39 9 47	3.585	0.0002	0.785		
	L Culmen	-28 -35 -35	3.402	0.0004	0.921		
2	L Middle Temporal Gyrus (BA 21)	-67 -25 -10	6.787	< 0.0001	<0.001	2743	0.004
	L Middle Temporal Gyrus (BA 21)	-61 -32 -7	6.308	< 0.0001	<0.001		
	L Inferior Temporal Gyrus (BA 20)	-48 -52 -13	4.492	< 0.0001	0.082		
3	L Supramarginal Gyrus (BA 22)	-58 -52 24	6.302	< 0.0001	<0.001	4499	0.001
	L Supramarginal Gyrus (BA 39)	-49 -53 32	5.786	< 0.0001	<0.001		
	L Inferior Parietal Lobule (BA 40)	-48 -55 47	5.554	< 0.0001	0.001		
	L Inferior Parietal Lobule (BA 40)	-66 -40 21	3.811	< 0.0001	0.556		
4	L Cerebellar Crus II	-48 -46 -41	5.084	< 0.0001	0.008	273	0.226

Peaks with significance p = 0.001 or less, uncorrected. Peaks at minimum distance 10 mm. Clu#: cluster number; Coord. (mm.): coordinates in Montreal Neurological Institute; p (uncorr.): significance value, uncorrected; p (corr.): significance value, peak-level corrected; k: cluster extent (in 1.5 mm voxels); p (cl.): significance value, cluster-level corrected.

Table A4. Forage trend high vs low. Interaction between time on task and reward, negative direction.

Clu #	Brain area	Coord. (mm.)	t	p (uncorr.)	p (corr.)	k	p (cl.)
1	L Precentral Gyrus (BA 6)	-31 -22 71	-12.729	< 0.0001	<0.001	25158	<0.001
	L Precentral Gyrus (BA 6)	-39 -19 65	-12.572	< 0.0001	<0.001		
	L Precentral Gyrus (BA 4)	-39 -16 48	-10.418	< 0.0001	<0.001		
	L Postcentral Gyrus (BA 43)	-49 -14 17	-7.668	< 0.0001	<0.001		
	L Superior Temporal Gyrus (BA 22)	-60 -11 2	-6.328	< 0.0001	<0.001		
	L Precentral Gyrus (BA 6)	-52 -4 26	-5.841	< 0.0001	<0.001		

	L Cingulate Gyrus (BA 24)	-9 5 48	-5.724	< 0.0001	<0.001		
	L Superior Frontal Gyrus (BA 6)	-18 2 72	-5.044	< 0.0001	0.010		
	L Caudate	-19 17 20	-4.838	< 0.0001	0.023		
	R Medial Frontal Gyrus (BA 6)	9 2 53	-4.728	< 0.0001	0.035		
	L Caudate	-18 8 26	-4.593	< 0.0001	0.055		
	L Cingulate Gyrus	-16 -22 44	-4.576	< 0.0001	0.058		
	L Medial Frontal Gyrus (BA 6)	-4 -7 59	-4.335	< 0.0001	0.138		
	L Precuneus (BA 7)	-19 -50 56	-4.089	< 0.0001	0.286		
	L Inferior Parietal Lobule (BA 5)	-28 -43 54	-4.031	< 0.0001	0.338		
	L Inferior Frontal Gyrus (BA 9)	-60 6 36	-3.908	< 0.0001	0.456		
2	R Culmen (BA 37)	19 -50 -22	-8.286	< 0.0001	<0.001	1415	0.014
3	L Lingual Gyrus (BA 18)	-13 -79 -7	-8.067	< 0.0001	<0.001	1461	0.013
4	L Inferior Temporal Gyrus (BA 20)	-37 -7 -37	-5.877	< 0.0001	<0.001	2488	0.004
	L Fusiform Gyrus (BA 36)	-28 2 -38	-4.986	< 0.0001	0.013		
	L Fusiform Gyrus (BA 20)	-52 -37 -28	-4.145	< 0.0001	0.243		
	L Parahippocampal Gyrus (BA 20)	-31 -20 -26	-3.533	0.0002	0.825		
5	R Uncus (BA 20)	28 2 -41	-5.653	< 0.0001	<0.001	1024	0.025
6	L Cuneus (BA 19)	-19 -91 29	-5.556	< 0.0001	0.001	5576	0.001
	L Middle Occipital Gyrus (BA 18)	-30 -97 6	-5.269	< 0.0001	0.003		
	L Middle Occipital Gyrus (BA 17)	-9 -103 12	-5.254	< 0.0001	0.004		
	L Primary Visual Cortex (BA 17)	-7 -106 -5	-5.129	< 0.0001	0.006		
	L Middle Occipital Gyrus (BA 19)	-46 -76 5	-5.092	< 0.0001	0.008		
	L Primary Visual Cortex (BA 17)	-1 -104 3	-5.030	< 0.0001	0.011		
	L Middle Occipital Gyrus (BA 18)	-21 -98 14	-4.733	< 0.0001	0.035		
	L Inferior Occipital Gyrus (BA 18)	-36 -92 -13	-4.137	< 0.0001	0.249		
	L Cuneus (BA 19)	-7 -91 38	-3.770	< 0.0001	0.595		
7	L Superior Frontal Gyrus (BA 9)	-34 47 38	-5.135	< 0.0001	0.006	573	0.076
	L Middle Frontal Gyrus (BA 8)	-34 39 45	-4.973	< 0.0001	0.013		
8	R Precentral Gyrus (BA 43)	61 -1 23	-4.879	< 0.0001	0.020	816	0.040
	R Precentral Gyrus (BA 6)	43 -10 38	-4.312	< 0.0001	0.148		
9	R Middle Occipital Gyrus (BA 18)	34 -94 12	-4.639	< 0.0001	0.047	485	0.100
	R Middle Occipital Gyrus (BA 18)	27 -101 0	-4.141	< 0.0001	0.246		
	R Cuneus (BA 18)	19 -104 -7	-3.823	< 0.0001	0.541		

Peaks with significance p = 0.001 or less, uncorrected. Peaks at minimum distance 10 mm. Clu#: cluster number; Coord. (mm.): coordinates in Montreal Neurological Institute; p (uncorr.): significance value, uncorrected; p (corr.): significance value, peak-level corrected; k: cluster extent (in 1.5 mm voxels); p (cl.): significance value, cluster-level corrected.

References

Abler, B., Walter, H., Erk, S., Kammerer, H., & Spitzer, M. (2006). Prediction error as a linear function of reward probability is coded in human nucleus accumbens. *NeuroImage*, *31*(2), 790-795. https://doi.org/10.1016/j.neuroimage.2006.01.001

Al-Hasani, R., Gowrishankar, R., Schmitz, G. P., Pedersen, C. E., Marcus, D. J., Shirley, S. E., Hobbs, T. E., Elerding, A. J., Renaud, S. J., Jing, M., Li, Y., Alvarez, V. A., Lemos, J. C., & Bruchas, M. R. (2021). Ventral tegmental area GABAergic inhibition of cholinergic interneurons in the ventral nucleus accumbens shell promotes reward reinforcement. *Nature Neuroscience*, *24*(10), 1414-1428. https://doi.org/10.1038/s41593-021-00898-2

Amunts, K., Kedo, O., Kindler, M., Pieperhoff, P., Mohlberg, H., Shah, N. J., Habel, U., Schneider, F., & Zilles, K. (2005). Cytoarchitectonic mapping of the human amygdala, hippocampal region and entorhinal cortex: intersubject variability and probability maps. *Anatomy and Embryology*, *210*(5-6), 343-352. https://doi.org/10.1007/s00429-005-0025-5

Aston-Jones, G., Rajkowski, J., Kubiak, P., & Alexinsky, T. (1994). Locus coeruleus neurons in monkey are selectively activated by attended cues in a vigilance task. *The Journal of Neuroscience*, *14*(7), 4467-4480.

Ballard, I. C., Murty, V. P., Carter, R. M., Macinnes, J. J., Huettel, S. A., & Adcock, R. A. (2011). Dorsolateral Prefrontal Cortex Drives Mesolimbic Dopaminergic Regions to Initiate Motivated Behavior. *Journal of Neuroscience*, *31*(28), 10340-10346. https://doi.org/10.1523/jneurosci.0895-11.2011

Barron, H. C., Garvert, M. M., & Behrens, T. E. J. (2016). Repetition suppression: a means to index neural representations using BOLD? *Philosophical Transactions of the Royal Society B: Biological Sciences*, *371*(1705), 20150355. https://doi.org/10.1098/rstb.2015.0355

Bates, D., Mächler, M., Bolker, B., & Walker, S. (2015). Fitting Linear Mixed-Effects Models Using lme4. *Journal of Statistical Software*, *67*(1), 1-48. https://doi.org/10.18637/jss.v067.i01

Berns, G. S., McClure, S. M., Pagnoni, G., & Montague, P. R. (2001). Predictability Modulates Human Brain Response to Reward. *The Journal of Neuroscience*, *21*(8), 2793-2798. https://doi.org/10.1523/jneurosci.21-08-02793.2001

Boksem, M. A. S., & Tops, M. (2008). Mental fatigue: Costs and benefits. *Brain Research Reviews*, *59*(1), 125-139. https://doi.org/10.1016/j.brainresrev.2008.07.001

Botvinick, M., & Braver, T. (2015). Motivation and Cognitive Control: From Behavior to Neural Mechanism. *Annual Review of Psychology*, *66*(1), 83-113. https://doi.org/10.1146/annurev-psych-010814-015044

Botvinick, M. M., Huffstetler, S., & McGuire, J. T. (2009). Effort discounting in human nucleus accumbens. *Cognitive, Affective, & Behavioral Neuroscience*, *9*(1), 16-27. https://doi.org/10.3758/CABN.9.1.16

Bouarab, C., Thompson, B., & Polter, A. M. (2019). VTA GABA Neurons at the Interface of Stress and Reward [Review]. *Frontiers in Neural Circuits*, *13*. https://doi.org/10.3389/fncir.2019.00078

Broussard, J. I. (2012). Posterior parietal cortex dynamically ranks topographic signals via cholinergic influence. *Front Integr Neurosci*, *6*, 32. https://doi.org/10.3389/fnint.2012.00032

Brown, M. T. C., Tan, K. R., O'Connor, E. C., Nikonenko, I., Muller, D., & Lüscher, C. (2012). Ventral tegmental area GABA projections pause accumbal cholinergic interneurons to enhance associative learning. *Nature*, *492*(7429), 452-456. https://doi.org/10.1038/nature11657

Coull, J. T. (1998). Neural correlates of attention and arousal: insights from electrophysiology, functional neuroimaging and psychopharmacology. *Progress in Neurobiology*, *55*(4), 343-361. https://doi.org/10.1016/S0301-0082(98)00011-2

Creed, M. C., Ntamati, N. R., & Tan, K. R. (2014). VTA GABA neurons modulate specific learning behaviors through the control of dopamine and cholinergic systems [Review]. *Frontiers in Behavioral Neuroscience*, *8*. https://doi.org/10.3389/fnbeh.2014.00008

Crouse, R. B., Kim, K., Batchelor, H. M., Girardi, E. M., Kamaletdinova, R., Chan, J., Rajebhosale, P., Pittenger, S. T., Role, L. W., Talmage, D. A., Jing, M., Li, Y., Gao, X.-B., Mineur, Y. S., & Picciotto, M. R. (2020). Acetylcholine is released in the basolateral amygdala in response to predictors of reward and enhances the learning of cue-reward contingency. *eLife*, *9*, e57335. https://doi.org/10.7554/eLife.57335

Davies, D. R., & Parasuraman, R. (1982). *The Psychology of Vigilance*. London: Academic Press.

Desikan, R. S., Ségonne, F., Fischl, B., Quinn, B. T., Dickerson, B. C., Blacker, D., Buckner, R. L., Dale, A. M., Maguire, R. P., Hyman, B. T., Albert, M. S., & Killiany, R. J. (2006). An automated labeling system for subdividing the human cerebral cortex on MRI scans into gyral based regions of interest. *NeuroImage*, *31*(3), 968-980. https://doi.org/10.1016/j.neuroimage.2006.01.021

Dutra, S. J., Marx, B. P., Mcglinchey, R., Degutis, J., & Esterman, M. (2018). Reward Ameliorates Posttraumatic Stress Disorder-Related Impairment in Sustained Attention. *Chronic Stress*, *2*, 247054701881240. https://doi.org/10.1177/2470547018812400

Eickhoff, S. B., Heim, S., Zilles, K., & Amunts, K. (2006). Testing anatomically specified hypotheses in functional imaging using cytoarchitectonic maps. *NeuroImage*, *32*(2), 570-582. https://doi.org/10.1016/j.neuroimage.2006.04.204

Eickhoff, S. B., Paus, T., Caspers, S., Grosbras, M.-H., Evans, A. C., Zilles, K., & Amunts, K. (2007). Assignment of functional activations to probabilistic cytoarchitectonic areas revisited. *NeuroImage*, *36*(3), 511-521. https://doi.org/10.1016/j.neuroimage.2007.03.060

Eickhoff, S. B., Stephan, K. E., Mohlberg, H., Grefkes, C., Fink, G. R., Amunts, K., & Zilles, K. (2005). A new SPM toolbox for combining probabilistic cytoarchitectonic maps and functional imaging data. *NeuroImage*, *25*(4), 1325-1335. https://doi.org/10.1016/j.neuroimage.2004.12.034

Eshel, N., Bukwich, M., Rao, V., Hemmelder, V., Tian, J., & Uchida, N. (2015). Arithmetic and local circuitry underlying dopamine prediction errors. *Nature*, *525*(7568), 243-246. https://doi.org/10.1038/nature14855

Esterman, M., Poole, V., Liu, G., & Degutis, J. (2017). Modulating Reward Induces Differential Neurocognitive Approaches to Sustained Attention. *Cerebral Cortex*, *27*(8), 4022-4032. https://doi.org/10.1093/cercor/bhw214

Esterman, M., Reagan, A., Liu, G., Turner, C., & DeGutis, J. (2014). Reward reveals dissociable aspects of sustained attention. *J Exp Psychol Gen*, *143*(6), 2287-2295. https://doi.org/10.1037/xge0000019

Frazier, J. A., Chiu, S., Breeze, J. L., Makris, N., Lange, N., Kennedy, D. N., Herbert, M. R., Bent, E. K., Koneru, V. K., Dieterich, M. E., Hodge, S. M., Rauch, S. L., Grant, P. E., Cohen, B. M., Seidman, L. J., Caviness, V. S., & Biederman, J. (2005). Structural brain magnetic resonance imaging of limbic and thalamic volumes in pediatric bipolar disorder. *The American journal of psychiatry*, *162*(7), 1256-1265. https://doi.org/10.1176/appi.ajp.162.7.1256

Goldstein, J. M., Seidman, L. J., Makris, N., Ahern, T., O'Brien, L. M., Caviness, V. S., Kennedy, D. N., Faraone, S. V., & Tsuang, M. T. (2007). Hypothalamic Abnormalities in Schizophrenia: Sex Effects and Genetic Vulnerability. *Biological Psychiatry*, *61*(8), 935-945. https://doi.org/10.1016/j.biopsych.2006.06.027

Grill-Spector, K., Henson, R., & Martin, A. (2006). Repetition and the brain: neural models of stimulus-specific effects. *Trends in Cognitive Sciences*, *10*(1), 14-23. https://doi.org/10.1016/j.tics.2005.11.006

Gritton, H. J., Howe, W. M., Mallory, C. S., Hetrick, V. L., Berke, J. D., & Sarter, M. (2016). Cortical cholinergic signaling controls the detection of cues. *Proceedings of the National Academy of Sciences*, *113*(8), E1089-E1097. https://doi.org/10.1073/pnas.1516134113

Hangya, B., Ranade, P., Sachin, Lorenc, M., & Kepecs, A. (2015). Central Cholinergic Neurons Are Rapidly Recruited by Reinforcement Feedback. *Cell*, *162*(5), 1155-1168. https://doi.org/10.1016/j.cell.2015.07.057

Harati, H., Barbelivien, A., Cosquer, B., Majchrzak, M., & Cassel, J. C. (2008). Selective cholinergic lesions in the rat nucleus basalis magnocellularis with limited damage in the medial septum specifically alter attention performance in the five-choice serial reaction time task. *Neuroscience*, *153*(1), 72-83. https://doi.org/10.1016/j.neuroscience.2008.01.031

Henson, R. N. A. (2003). Neuroimaging studies of priming. *Progress in Neurobiology*, *70*(1), 53-81. https://doi.org/10.1016/S0301-0082(03)00086-8

Howe, W. M., Berry, A. S., Francois, J., Gilmour, G., Carp, J. M., Tricklebank, M., Lustig, C., & Sarter, M. (2013). Prefrontal Cholinergic Mechanisms Instigating Shifts from Monitoring for Cues to Cue-Guided Performance: Converging Electrochemical and fMRI Evidence from Rats and Humans. *The Journal of Neuroscience*, *33*(20), 8742-8752. https://doi.org/10.1523/jneurosci.5809-12.2013

Huber, D., Rabl, L., Orsini, C., Labek, K., & Viviani, R. (2024). The fMRI global signal and its association with the signal from cranial bone. *NeuroImage*, *297*, 120754. https://doi.org/10.1016/j.neuroimage.2024.120754

Kahneman, D. (1973). *Attention and effort* (Vol. 1063). Englewood Cliffs, NJ: Prentice-Hall.

Kedo, O., Zilles, K., Palomero-Gallagher, N., Schleicher, A., Mohlberg, H., Bludau, S., & Amunts, K. (2018). Receptor-driven, multimodal mapping of the human amygdala. *Brain Structure and Function*, *223*(4), 1637-1666. https://doi.org/10.1007/s00429-017-1577-x

Keren, N. I., Lozar, C. T., Harris, K. C., Morgan, P. S., & Eckert, M. A. (2009). In vivo mapping of the human locus coeruleus. *NeuroImage*, *47*(4), 1261-1267. https://doi.org/10.1016/j.neuroimage.2009.06.012

Kool, W., McGuire, J. T., Rosen, Z. B., & Botvinick, M. M. (2010). Decision making and the avoidance of cognitive demand. *J Exp Psychol Gen*, *139*(4), 665-682. https://doi.org/10.1037/a0020198

Koulousakis, P., Andrade, P., Visser-Vandewalle, V., & Sesia, T. (2019). The Nucleus Basalis of Meynert and Its Role in Deep Brain Stimulation for Cognitive Disorders: A Historical Perspective. *Journal of Alzheimer's Disease*, *69*, 905-919. https://doi.org/10.3233/JAD-180133

Kurniawan, I. T., Guitart-Masip, M., Dayan, P., & Dolan, R. J. (2013). Effort and Valuation in the Brain: The Effects of Anticipation and Execution. *The Journal of Neuroscience*, *33*(14), 6160-6169. https://doi.org/10.1523/jneurosci.4777-12.2013

Kurzban, R. (2016). The sense of effort. *Current Opinion in Psychology*, *7*, 67-70. https://doi.org/10.1016/j.copsyc.2015.08.003

Kurzban, R., Duckworth, A., Kable, J. W., & Myers, J. (2013). An opportunity cost model of subjective effort and task performance. *Behavioral and Brain Sciences*, *36*(6), 661-679. https://doi.org/10.1017/s0140525x12003196

Labek, K., & Viviani, R. (2025, in press). Functional imaging of time on task and habituation in passive exposure to faces with emotional expression. *Neuroreport*.

Langner, R., & Eickhoff, S. B. (2013). Sustaining attention to simple tasks: A meta-analytic review of the neural mechanisms of vigilant attention. *Psychological Bulletin*, *139*(4), 870-900. https://doi.org/10.1037/a0030694

Li, J., McClure, S. M., King-Casas, B., & Read Montague, P. (2006). Policy Adjustment in a Dynamic Economic Game. *PLOS ONE*, *1*(1), e103. https://doi.org/10.1371/journal.pone.0000103

Liu, R., Crawford, J., Callahan, P. M., Terry, A. V., Constantinidis, C., & Blake, D. T. (2018). Intermittent stimulation in the nucleus basalis of meynert improves sustained attention in rhesus monkeys. *Neuropharmacology*, *137*, 202-210. https://doi.org/10.1016/j.neuropharm.2018.04.026

Mackworth, N. H. (1948). The Breakdown of Vigilance during Prolonged Visual Search. *Quarterly Journal of Experimental Psychology*, *1*(1), 6-21. https://doi.org/10.1080/17470214808416738

Mackworth, N. H. (1950). *Researches on the measurement of human performance. (Med. Res. Council, Special Rep. Ser. No. 268.)*. His Majesty"s Stationery Office.

Makris, N., Goldstein, J. M., Kennedy, D., Hodge, S. M., Caviness, V. S., Faraone, S. V., Tsuang, M. T., & Seidman, L. J. (2006). Decreased volume of left and total anterior insular lobule in schizophrenia. *Schizophrenia Research*, *83*(2), 155-171. https://doi.org/10.1016/j.schres.2005.11.020

Martinez-Rubio, C., Paulk, A. C., Mcdonald, E. J., Widge, A. S., & Eskandar, E. N. (2018). Multimodal Encoding of Novelty, Reward, and Learning in the Primate Nucleus Basalis of Meynert. *The Journal of Neuroscience*, *38*(8), 1942-1958. https://doi.org/10.1523/jneurosci.2021-17.2017

Martinez, V., & Sarter, M. (2004). Lateralized attentional functions of cortical cholinergic inputs. *Behav Neurosci*, *118*(5), 984-991. https://doi.org/10.1037/0735-7044.118.5.984

Massar, S. A., Lim, J., Sasmita, K., & Chee, M. W. (2016). Rewards boost sustained attention through higher effort: A value-based decision making approach. *Biol Psychol*, *120*, 21-27. https://doi.org/10.1016/j.biopsycho.2016.07.019

McClure, S. M., Berns, G. S., & Montague, P. R. (2003). Temporal Prediction Errors in a Passive Learning Task Activate Human Striatum. *Neuron*, *38*(2), 339-346. https://doi.org/10.1016/S0896-6273(03)00154-5

McGaughy, J., Dalley, J. W., Morrison, C. H., Everitt, B. J., & Robbins, T. W. (2002). Selective Behavioral and Neurochemical Effects of Cholinergic Lesions Produced by Intrabasalis Infusions of 192 IgG-Saporin on Attentional Performance in a Five-Choice Serial Reaction Time Task. *The Journal of Neuroscience*, *22*(5), 1905-1913. https://doi.org/10.1523/jneurosci.22-05-01905.2002

McGaughy, J., Decker, M. W., & Sarter, M. (1999). Enhancement of sustained attention performance by the nicotinic acetylcholine receptor agonist ABT-418 in intact but not basal forebrain-lesioned rats. *Psychopharmacology*, *144*(2), 175-182. https://doi.org/10.1007/s002130050991

Mcguire, J. T., & Botvinick, M. M. (2010). Prefrontal cortex, cognitive control, and the registration of decision costs. *Proceedings of the National Academy of Sciences*, *107*(17), 7922-7926. https://doi.org/10.1073/pnas.0910662107

Mesulam, M. M. (2004). The cholinergic innervation of the human cerebral cortex. In *Progress in Brain Research* (Vol. 145, pp. 67-78). Elsevier. https://doi.org/10.1016/S0079-6123(03)45004-8

Mesulam, M. M. (2013). Cholinergic circuitry of the human nucleus basalis and its fate in Alzheimer's disease. *Journal of Comparative Neurology*, *521*(18), 4124-4144. https://doi.org/10.1002/cne.23415

Mesulam, M. M., Mufson, E. J., Levey, A. I., & Wainer, B. H. (1983). Cholinergic innervation of cortex by the basal forebrain: cytochemistry and cortical connections of the septal area, diagonal band nuclei, nucleus basalis (substantia innominata), and hypothalamus in the rhesus monkey. *J Comp Neurol*, *214*(2), 170-197. https://doi.org/10.1002/cne.902140206

Montague, P., Dayan, P., & Sejnowski, T. (1996). A framework for mesencephalic dopamine systems based on predictive Hebbian learning. *The Journal of Neuroscience*, *16*(5), 1936-1947. https://doi.org/10.1523/jneurosci.16-05-01936.1996

Morales, M., & Margolis, E. B. (2017). Ventral tegmental area: cellular heterogeneity, connectivity and behaviour. *Nature Reviews Neuroscience*, *18*(2), 73-85. https://doi.org/10.1038/nrn.2016.165

Murty, V. P., Shermohammed, M., Smith, D. V., Carter, R. M., Huettel, S. A., & Adcock, R. A. (2014). Resting state networks distinguish human ventral tegmental area from substantia nigra. *NeuroImage*, *100*, 580-589. https://doi.org/10.1016/j.neuroimage.2014.06.047

Norman, D. A., & Shallice, T. (1986). Attention to Action: Willed and automatic control of behavior. In R. J. Davidson, G. E. Schwartz, & D. Shapiro (Eds.), *Consciousness and Self-Regulation: Advances in Research and Theory Volume 4* (pp. 1-18). Springer US. https://doi.org/10.1007/978-1-4757-0629-1_1

O'Doherty, J. P., Dayan, P., Friston, K., Critchley, H., & Dolan, R. J. (2003). Temporal difference models and reward-related learning in the human brain. *Neuron*, *38*(2), 329-337. https://doi.org/10.1016/s0896-6273(03)00169-7

Oken, B. S., Salinsky, M. C., & Elsas, S. M. (2006). Vigilance, alertness, or sustained attention: physiological basis and measurement. *Clinical Neurophysiology*, *117*(9), 1885-1901. https://doi.org/10.1016/j.clinph.2006.01.017

Parasuraman, R., & Davies, D. R. (1984). *Varieties of attention*. Academic Press.

Paus, T. (2000). Functional anatomy of arousal and attention systems in the human brain. In *Progress in Brain Research* (Vol. 126, pp. 65-77). Elsevier. https://doi.org/10.1016/S0079-6123(00)26007-X

Paus, T., Zatorre, R. J., Hofle, N., Caramanos, Z., Gotman, J., Petrides, M., & Evans, A. C. (1997). Time-related changes in neural systems underlying attention and arousal during the performance of an auditory vigilance task. *J Cogn Neurosci*, *9*(3), 392-408. https://doi.org/10.1162/jocn.1997.9.3.392

Posner, M. I., & Boies, S. J. (1971). Components of attention. *Psychological Review*, *78*(5), 391-408. https://doi.org/10.1037/h0031333

Race, E. A., Shanker, S., & Wagner, A. D. (2009). Neural Priming in Human Frontal Cortex: Multiple Forms of Learning Reduce Demands on the Prefrontal Executive System. *Journal of Cognitive Neuroscience*, *21*(9), 1766-1781. https://doi.org/10.1162/jocn.2009.21132

Riccio, C. A., Reynolds, C. R., Lowe, P., & Moore, J. J. (2002). The continuous performance test: a window on the neural substrates for attention? *Archives of Clinical Neuropsychology*, *17*(3), 235-272. https://doi.org/10.1016/S0887-6177(01)00111-1

Richardson, R. T., & DeLong, M. R. (1986). Nucleus basalis of Meynert neuronal activity during a delayed response task in monkey. *Brain Research*, *399*(2), 364-368. https://doi.org/10.1016/0006-8993(86)91529-5

Robertson, I. H., & O'Connell, R. (2010). Vigilant attention. In A. C. Nobre & J. T. Coull (Eds.), *Attention and Time* (pp. 79-88). Oxford University Press. https://doi.org/10.1093/acprof:oso/9780199563456.003.0006

Rutledge, R. B., Dean, M., Caplin, A., & Glimcher, P. W. (2010). Testing the Reward Prediction Error Hypothesis with an Axiomatic Model. *The Journal of Neuroscience*, *30*(40), 13525-13536. https://doi.org/10.1523/jneurosci.1747-10.2010

Salamone, D., John, & Correa, M. (2012). The Mysterious Motivational Functions of Mesolimbic Dopamine. *Neuron*, *76*(3), 470-485. https://doi.org/10.1016/j.neuron.2012.10.021

Salamone, J. D., Correa, M., Farrar, A., & Mingote, S. M. (2007). Effort-related functions of nucleus accumbens dopamine and associated forebrain circuits. *Psychopharmacology*, *191*(3), 461-482. https://doi.org/10.1007/s00213-006-0668-9

Sarter, M., & Bruno, J. P. (2002). Vigilance. In V. S. Ramachandran (Ed.), *Encyclopedia of the Human Brain* (pp. 687-699). Academic Press. https://doi.org/10.1016/B0-12-227210-2/00357-5

Sarter, M., Gehring, W. J., & Kozak, R. (2006). More attention must be paid: The neurobiology of attentional effort. *Brain Research Reviews*, *51*(2), 145-160. https://doi.org/10.1016/j.brainresrev.2005.11.002

Sarter, M., Givens, B., & Bruno, J. P. (2001). The cognitive neuroscience of sustained attention: where top-down meets bottom-up. *Brain Research Reviews*, *35*(2), 146-160. https://doi.org/10.1016/S0165-0173(01)00044-3

Schacter, D. L., & Buckner, R. L. (1998). Priming and the Brain. *Neuron*, *20*(2), 185-195. https://doi.org/10.1016/s0896-6273(00)80448-1

Schacter, D. L., Dobbins, I. G., & Schnyer, D. M. (2004). Specificity of priming: a cognitive neuroscience perspective. *Nature Reviews Neuroscience*, *5*(11), 853-862. https://doi.org/10.1038/nrn1534

Schultz, W. (1998). Predictive Reward Signal of Dopamine Neurons. *Journal of Neurophysiology*, *80*(1), 1-27. https://doi.org/10.1152/jn.1998.80.1.1

Seymour, B., Daw, N., Dayan, P., Singer, T., & Dolan, R. (2007). Differential Encoding of Losses and Gains in the Human Striatum. *The Journal of Neuroscience*, *27*(18), 4826-4831. https://doi.org/10.1523/jneurosci.0400-07.2007

Shallice, T., & Burgess, P. (1996). The domain of supervisory processes and temporal organization of behaviour. *Philos Trans R Soc Lond B Biol Sci*, *351*(1346), 1405-1411; discussion 1411-1402. https://doi.org/10.1098/rstb.1996.0124

Shenhav, A., Botvinick, M., Matthew, & Cohen, D., Jonathan. (2013). The Expected Value of Control: An Integrative Theory of Anterior Cingulate Cortex Function. *Neuron*, *79*(2), 217-240. https://doi.org/10.1016/j.neuron.2013.07.007

Shenhav, A., Cohen, J. D., & Botvinick, M. M. (2016). Dorsal anterior cingulate cortex and the value of control. *Nature Neuroscience*, *19*(10), 1286-1291. https://doi.org/10.1038/nn.4384

Shenhav, A., Musslick, S., Lieder, F., Kool, W., Griffiths, T. L., Cohen, J. D., & Botvinick, M. M. (2017). Toward a Rational and Mechanistic Account of Mental Effort. *Annual Review of Neuroscience*, *40*(1), 99-124. https://doi.org/10.1146/annurev-neuro-072116-031526

Stöcker, T., Kellermann, T., Schneider, F., Habel, U., Amunts, K., Pieperhoff, P., Zilles, K., & Shah, N. J. (2006). Dependence of amygdala activation on echo time: Results from olfactory fMRI experiments. *NeuroImage*, *30*(1), 151-159. https://doi.org/10.1016/j.neuroimage.2005.09.050

Tashakori-Sabzevar, F., & Ward, R. D. (2018). Basal Forebrain Mediates Motivational Recruitment of Attention by Reward-Associated Cues. *Frontiers in Neuroscience*, *12*. https://doi.org/10.3389/fnins.2018.00786

Timmers, D. (2014). Chapter Six - Treating Attention Deficits and Impulse Control. In D. S. Cantor & J. R. Evans (Eds.), *Clinical Neurotherapy* (pp. 139-169). Academic Press. https://doi.org/10.1016/B978-0-12-396988-0.00006-4

Tobler, P. N., O'Doherty, J. P., Dolan, R. J., & Schultz, W. (2006). Human Neural Learning Depends on Reward Prediction Errors in the Blocking Paradigm. *Journal of Neurophysiology*, *95*(1), 301-310. https://doi.org/10.1152/jn.00762.2005

Tomporowski, P. D., & Tinsley, V. F. (1996). Effects of memory demand and motivation on sustained attention in young and older adults. *Am J Psychol*, *109*(2), 187-204.

Usher, M., Cohen, J. D., Servan-Schreiber, D., Rajkowski, J., & Aston-Jones, G. (1999). The Role of Locus Coeruleus in the Regulation of Cognitive Performance. *Science*, *283*(5401), 549-554. https://doi.org/10.1126/science.283.5401.549

Viviani, R., Dommes, L., Bosch, J., Steffens, M., Paul, A., Schneider, K. L., Stingl, J. C., & Beschoner, P. (2020). Signals of anticipation of reward and of mean reward rates in the human brain. *Scientific Reports*, *10*(1). https://doi.org/10.1038/s41598-020-61257-y

Viviani, R., Dommes, L., Bosch, J. E., & Labek, K. (2020). Segregation, connectivity, and gradients of deactivation in neural correlates of evidence in social decision making. *NeuroImage*, *223*, 117339. https://doi.org/10.1016/j.neuroimage.2020.117339

Viviani, R., Messina, I., Bosch, J. E., Dommes, L., Paul, A., Schneider, K. L., Scholl, C., & Stingl, J. C. (2020). Effects of genetic variability of CYP2D6 on neural substrates of sustained attention during on-task activity. *Translational Psychiatry*, *10*(1). https://doi.org/10.1038/s41398-020-01020-z

Walton, M. E., & Bouret, S. (2019). What Is the Relationship between Dopamine and Effort? *Trends in Neurosciences*, *42*(2), 79-91. https://doi.org/10.1016/j.tins.2018.10.001

Walton, M. E., Kennerley, S. W., Bannerman, D. M., Phillips, P. E. M., & Rushworth, M. F. S. (2006). Weighing up the benefits of work: Behavioral and neural analyses of effort-related decision making. *Neural Networks*, *19*(8), 1302-1314. https://doi.org/10.1016/j.neunet.2006.03.005

Warm, J. S., Parasuraman, R., & Matthews, G. (2008). Vigilance Requires Hard Mental Work and Is Stressful. *Human Factors*, *50*(3), 433-441. https://doi.org/10.1518/001872008x312152

Wickham, H. (2016). *ggplot2: Elegant Graphics for Data Analysis*. Springer-Verlag New York. https://ggplot2.tidyverse.org

Wickham, H., François, R., Henry, L., Müller, K., & Vaughan, D. (2023). *dplyr: A Grammar of Data Manipulation*. In (Version 1.1.4) [R package]. https://CRAN.R-project.org/package=dplyr

Wickham, H., Vaughan, D., & Girlich, M. (2023). *tidyr: Tidy Messy Data*. In (Version 1.3.0) [R package]. https://CRAN.R-project.org/package=tidyr

Wiggs, C. L., & Martin, A. (1998). Properties and mechanisms of perceptual priming. *Current Opinion in Neurobiology*, *8*(2), 227-233. https://doi.org/10.1016/s0959-4388(98)80144-x

Wolpe, N., Holton, R., & Fletcher, P. C. (2024). What Is Mental Effort: A Clinical Perspective. *Biological Psychiatry*, *95*(11), 1030-1037. https://doi.org/10.1016/j.biopsych.2024.01.022

Zaborszky, L., Hoemke, L., Mohlberg, H., Schleicher, A., Amunts, K., & Zilles, K. (2008). Stereotaxic probabilistic maps of the magnocellular cell groups in human basal forebrain. *NeuroImage*, *42*(3), 1127-1141. https://doi.org/10.1016/j.neuroimage.2008.05.055

Zhou, W.-L., Kim, K., Ali, F., Pittenger, S. T., Calarco, C. A., Mineur, Y. S., Ramakrishnan, C., Deisseroth, K., Kwan, A. C., & Picciotto, M. R. (2022). Activity of a direct VTA to ventral pallidum GABA pathway encodes unconditioned reward value and sustains

motivation for reward. *Science Advances*, *8*(42), eabm5217. https://doi.org/10.1126/sciadv.abm5217